University of Stavanger

Faculty of Science and Technology

MASTER'S THESIS

Study program/ Specialization: Konstruksjoner og materialer – master degree	Spring semester, 2013 Open access
Writer: Christoffer Leidland Andersen	Christoffer L. Andersen (Writer's signature)
Faculty supervisor: Hirpa Lemu Gelgele External supervisor(s):	
Title of thesis: ***Modeling, analysis and testing of the Steering system in a Formula Student car FS_UiS2013***	
Credits (ECTS): 30	
Key words: Steering rack configuration Tie rods design Offset arm design MSC Adams analysis Cost report	Pages: 60 + enclosure: 53 Stavanger, 24.06/2013 Date/year

PREFACE

This Master Thesis are considering the design, analysis and testing of the steering system on a Formula Student racing car. The car is built at the University of Stavanger during the spring 2013 and will compete at the Silverstone Circuit in July 2013.

I would like to thank the following persons:

Jan Kåre Bording, chief engineer at the workshop at University of Stavanger, for his helpful advice and support during the project

Hirpa Lemu Gelgele, associate professor at the University of Stavanger, for being my supervisor during the project and for his help and support during the project

Rosenberg Worley Parsons Group for the decision to be our main sponsor and helping us financially to achieve our goals with the car

Stavanger, 24.06-2013

Christoffer Leidland Andersen

Romertal

Table of Contents

List of figures

SUMMARY

The University of Stavanger (UiS) is competing in a Formula Student competition at Silverstone in spring 2013 with a Formula Student racing car. This Master Thesis aims to design, analyze and test the steering system of the racing car. The car is built during the process of writing the thesis.

A manual steering system was preferred as the weight of the car is low and to reduce the risk of spillage due to the hydraulic pump that would be necessary with a power-assisted steering system. With an electrical driven system, additional weight would be added with an extra or heavier battery.

The car was designed for optimal performance in the skid-pad event with a reversed-Ackermann design. The Ackermann angle of the offset arm was set to 39.3 degrees giving the outer wheel an angle of 13 degrees and the inner wheel an angle of 11 degrees in a turn with a radius of 7583 mm.

The steering rack was placed in a far-front position to avoid big buildups of momentum during driving. The tie rods were angled at a same angle as the lower a-arm to reduce the bump steer.

The biggest lateral force occurred during cornering and this was used for the design of the tie rods. During the analysis of the system, a bigger force occurred on the tie rod during braking, and the system was rechecked and approved for this force.

MSC Adams was used in the design and analysis phase to consider the functionality and behavior of the steering system.

Due to limitations in the budget, the team used the same Hoosier tires as last year. The 2014 team should pay to get access to the Milliken Research Associates, which is a tire test consortium, to obtain tire test data and make a decision if another brand of tire would fit the project better. The budget for the steering system should also be raised to be able to buy a lighter steering rack to lower the total weight of the steering system. The total weight of the 2013 steering system is 3957.8 grams.

The 2013 budget for the steering system was set to 5500 NOK. A new quick release mechanism had to be bought which raised the total amount for the system to 6228.56 NOK. It should be possible to use the same quick release mechanism next year.

1 INTRODUCTION

1.1 Background

The University of Stavanger (UiS) is participating in a Formula Student competition in the United Kingdom (UK) at the Silverstone circuit from 2nd to 7th July, 2013. The Formula Student (FS) is run by the Institution of Mechanical Engineers (IMechE) and is arranged each July at the Silverstone. It is a competition that challenges young student-engineers from all over the world to design, build and compete with a single-seat racing car.

In 1981, the Society of Automotive Engineers (SAE) started to run competitions in the United States. In 1998 it was held a demonstration event in the United Kingdom (UK) where two US cars and two UK cars competed. Since then, the competition has been arranged every year in the UK and at the Silverstone circuit since 2007.

Formula Student has four classes:

- Class 1: The teams design, manufacture and race a fully working car
- Class 1a: The same as class 1, but the cars are running on alternative fuel
- Class 2: Teams have planned and designed, but not build a car, and are judged on business presentation, design and cost
- Class 2a: The same as class 2, but the teams have planned an alternative fuelled car

The University of Stavanger (UiS) attended for the first time the class 1 group at Silverstone in July 2012. With more than 3000 students from 34 countries and 132 cars the competition was hard, giving a total score of 111.2 points and a 84th place where the best team scored 850.5 points.

1.2 The Objective

The objective for the competition is to produce a prototype racing car for autocross and sprint racing within the design rules set by the competition rules. The teams have to assume that a manufacturing firm has engaged them, and that the customer is a non-professional racer who demands the car to be low in cost, reliable and easy to maintain. To manage this, the students have to work in teams and gain management and marketing skills as well as technical and communication skills. During the development and manufacturing process, the teams have to upload documentations to the judges to identify their goals and to get clearance for their design. Cost analysis is a vital part of the process which has to be presented at the competition. By doing these steps the students learn the importance of keeping the project within the budget and to the deadlines.

The teams will go through the following testing at the competition days:

Static events:

- Design, cost and presentation judging
- Technical and safety scrutineering
- Tilt test
- Brake and noise test

Dynamic events:

- Skid pad (driving in a figure of 8)
- Sprint
- Acceleration
- Endurance and fuel economy

1.3 The Aim

This Master Thesis aims to design, analyze and build a steering system for the formula student 2013 racing car (appendix A). During the process of writing the Master Thesis, a fully functional system has also been manufactured, tested and assembled on the racing car. During the project, economical funding from sponsors has made an upper limit of what is achievable when it comes to material choice, weight etc. of the components chosen.

MSC Adams has been used in the analyzing phase for multi-body simulation of the steering system.

1.4 Conclusions

1.5 Recommendations

2 TIRE

There are three main different construction types of tires used in the car industry:

- *Radial tires:*
  A series of cord plies, which are layers embedded in the rubber to strengthen it and hold its shape, are arranged perpendicular or radial to the direction of travel. This makes the tire act like a spring with flexibility and better comfort. In addition, belts are added closer to the direction of travel to add further stiffness.

- *Bias belted tires:*
  Stabilizer belts are bonded to two or more bias-plies, directly beneath the tread.

- *Bias ply tires:*
  Plies extend diagonally from bead to bead with other plies laid in opposing angles making a crisscross pattern. The tread, which is the area of the tire that comes in contact with the road surface, are applied onto the crisscross pattern.

2.1 Lateral force

A tire will experience lateral force. According to SAE J670, “a lateral tire force originates at the “center” of the tire contact with the road, and is perpendicular to the direction in which the wheel is headed.” The centroid of the lateral force is aft of the center of the print. The print is the area of the tread of the tire that is in contact with the ground at any moment.

2.2 Pneumatic trail

The distance from the center of the print to where the lateral force is acting is called the pneumatic trail. Pneumatic trail is generated when the tire is subjected to side forces as in cornering, and is greater towards the rear of the contact patch due to lateral force building up along the length of the patch. This creates a aligning torque on the tire that tends to steer it in the direction in which it is travelling. The resultant force will occur behind the center of the contact patch. As it occurs at a distance to the rear from the center patch it can be seen on as the moment arm through which the lateral force acts.

Pneumatic trail can be expressed as

$$t_p = \frac{M_Z}{F_Y} \qquad \text{(Equation 3.1)}$$

where
M_Z: Self-aligning torque [Nm]
F_Y: Lateral Force [N]

As the slip angle increases, the pneumatic trail and aligning torque will decrease as more of the rear contact patch starts to slide laterally. The footprint is sliding and hence got less ability to stabilize the wheel.

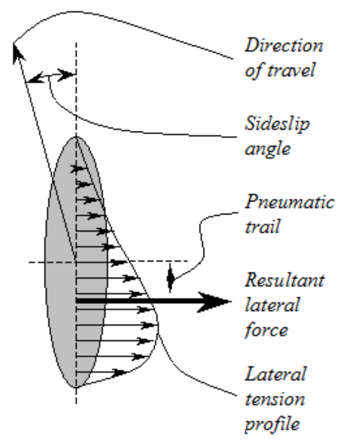

Figure 2-1: The pneumatic trail distribution

The pneumatic trail is a good source of telling when the breakaway would occur and that the front wheels are near the limits before sliding starts.

2.3 Mechanical trail

The caster angle gives a mechanical trail which is fixed by the steering and suspension geometry.

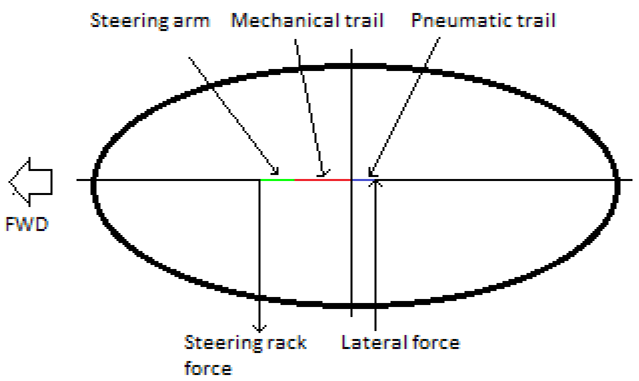

Figure 2-2: Mechanical and pneumatic trail on a tire

The mechanical trail is expressed by

$$Mechanical\ trail = \tan(\alpha) * R \qquad \text{(Equation 3.2)}$$

where
α: caster angle [degrees]
R: Radius of tire [mm]

2.4 Slip angle

The angle between a wheels actual direction of travel and the direction towards which it is pointing is called the slip angle.

3 STEERING SYSTEM

The steering system plays an important role for the vehicle as it is the "interface" between the driver and the vehicle. The driver turns the steering wheel which will rotate the steering column and give further movement in the steering rack. The motion is then transmitted to the wheels by the tie rods.

The design and type of the steering rack depends on the system chosen. The steering systems used are divided into power assisted and manual steering systems, each designed to help the driver to turn easily for optimal performance with different configuration of the vehicle.

3.1 Power Assisted Steering Systems

Power assisted steering systems are used to amplify the turning moment applied to the steering wheels for heavier vehicles which might be hard to turn with a manually steering system at low speeds. This is practical when the car is at a standstill and the wheels have to be turned, i.e. when parking.

A power assisted steering system is supported by a hydraulic pump driven by the motor which directs pressurized oil, a boost, to the steering gear and helps to push or pull the rack in either of the directions. The boost is applied to the steering linkage or the steering gear. A flow control valve limits the fluid flow to the cylinder, and a pressure relief valve controls the pressure.

The system can also be electrical driven. This is more efficient as the electric power steering only needs to assist when wheels are turned and are not run constantly with the engine as the hydraulically driven system. It also works even if the motor is not running and by the elimination of the pump, hoses and fluids the weight is reduced. There is no leakage of fluids and it runs quieter as there is no pump.

3.1.1 Power Assisted Rack and Pinion

The rack and pinion gear system is assisted by a pump connected to the engine and is run along with the engine. The pump is pumping fluid from a reservoir, through a controlling valve and into the system, as seen in figure 4-1.

The rack contains a cylinder with a piston and two fluid ports. By applying pressurized fluid to one of the sides of the piston forces the piston to move, which will move the rack.

As the pump is connected to the engine it only works when the engine is running. This is the reason why it is hard to turn the steering wheel when the car is turned off.

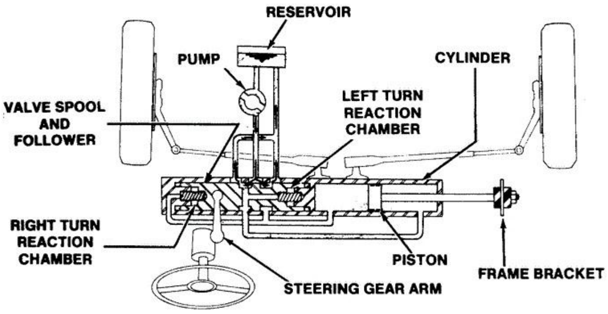

Figure 3-1: Power assisted rack and pinion

3.2 Manual Steering Systems

The manual steering systems are used on light weighted vehicles, or vehicles which have the biggest distribution of mass on the rear wheels and can be easily turned with manual steering at low speed. The systems are fast and accurate and it provides a reliable design.

However, it will become more difficult to handle the vehicle at low speed if wider tires are used or more weight is distributed to the front wheels. These concerns play a big role when analyzing if manual steering should be used.

There are different types of manual steering gear systems:

- Worm and roller
- Worm and sector
- Worm and nut
- Cam and lever
- Rack and pinion

3.2.1 Worm and Roller

The worm and roller gear has a connection between the worm and the roller, and the roller is supported by a roller bearing, as seen in figure 4-2. When the steering wheel turns the steering shaft, the worm is rotated which turns the roller. As a result of this motion, the sector and pitman arm shaft rotates.

The worm has a hourglass shape for variable steering ratio and better contact for the worm and roller. The variable steering ratio will result that the wheels turns faster at some positions than others. This will provide more steering control at the center of the worm, and more rapid steering as the wheels are turned.

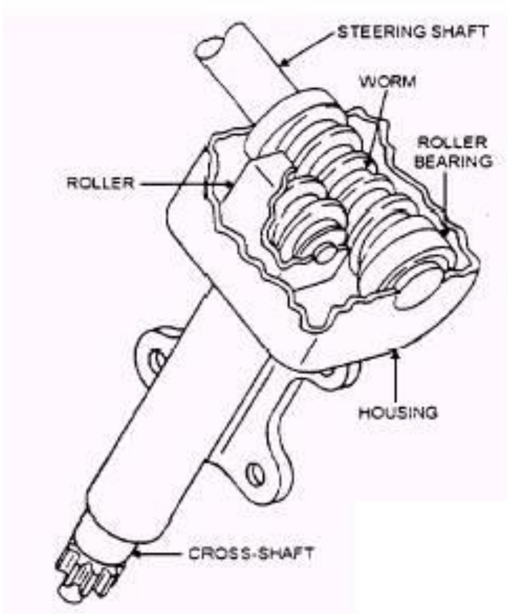

Figure 3-2: Worm and roller steering gear system

3.2.2 Worm and Sector

The worm and sector steering gear is shown in figure 4-3. The pitman arm shaft carries the sector gear. As the steering wheel rotates, the worm on the steering gear shaft rotates which rotates the sector and the pitman arm.

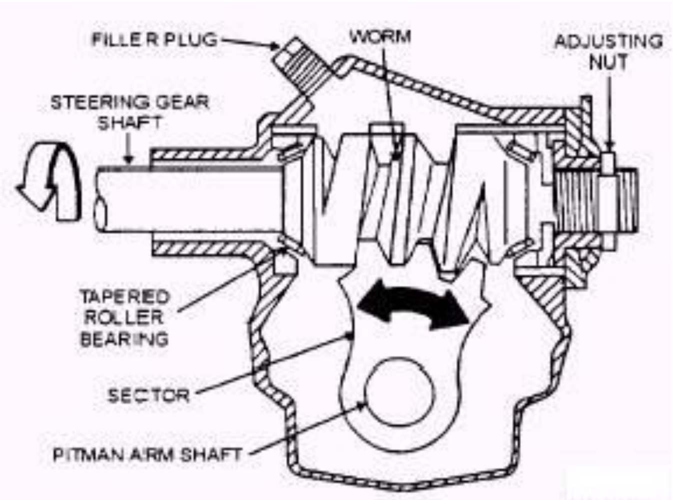

Figure 3-3: Worm and sector steering gear system

3.2.3 Worm and Nut

The worm and nut steering gear comes in different combinations where the recirculating ball is the most common type as shown in figure 4-4. The recirculation ball combination offers the connection of the nut on a row of balls on the worm gear to reduce friction. Ball guides returns the balls as the nut moves up and down. The ball nut is shaped to fit the sector gear.

When the steering wheel is turned, the steering shaft rotates along with the worm gear fitted at the end of it. The recirculation balls starts to move, and this moves the ball nut up and down along the worm. This turns the pitman arm.

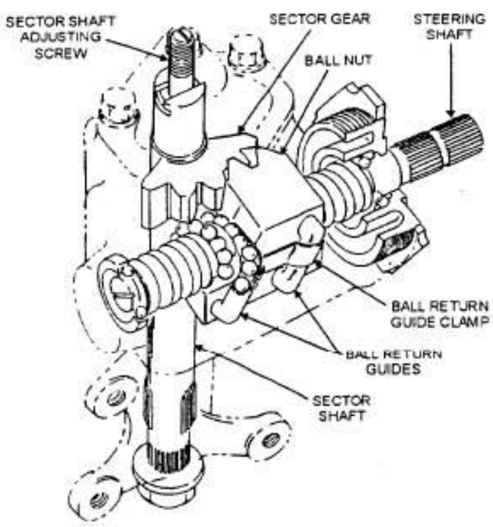

Figure 3-4: Worm and nut steering gear system

3.2.4 Cam and Lever

In the cam and lever gear, two studs are connected on the lever and engage the cam, figure 4-5. As the steering wheel is turned, the steering shaft will rotate and move the studs back and forth which move the lever back and forth. This will cause a rotation in the pitman arm. The lever is increased in angle compared to the cam, which will result in a more rapid move of the lever as it nears the ends, as in the worm and nut gear.

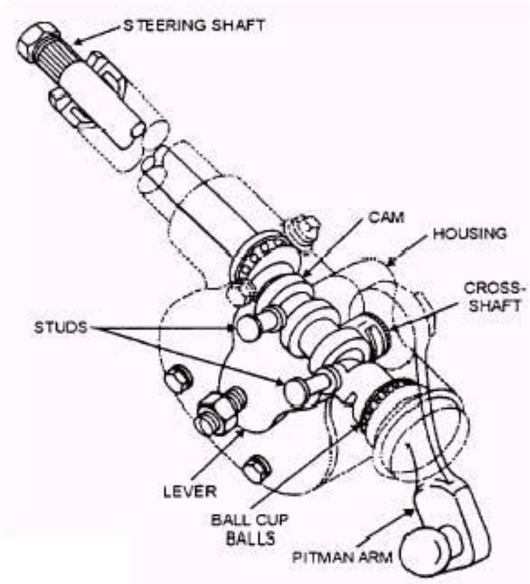

Figure 3-5: Cam and lever steering gear system

3.2.5 Rack and Pinion

In the rack and pinion gear, the rotating steering wheel and steering shaft rotates the pinion gear at the end of the steering shaft, figure 4-6. The rack is fitted to the pinion and as the pinion rotates, the rotation motion is changed to transverse movement of the rack gear and moves it to one of the sides. The tie rods at the ends of the rack, which are connected to the wheels, are pushed or pulled which turns the wheels.

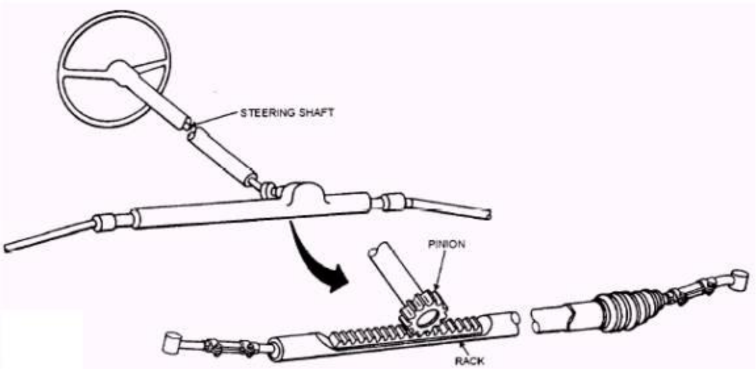

Figure 3-6: Rack and pinion steering gear system

The teeth on the rack can be either linear or variable. With a linear rate there is the same amount of teeth over the whole area which makes the wheels to respond the same regardless of the angle. With a variable rate the rack has closely packed teeth at the center and the distance between the teeth widens towards the ends. The result is better adjustment when driving straight and bigger respond when doing sharp turning.

3.3 Stability and Control

The handling, stability and control of the vehicle are influenced by many factors which have to be considered. I.e. the caster angle cannot be changed after the suspension system has been designed and mounted on the vehicle. The caster angle will affect the mechanical trail which will affect the response and feeling between the driver and the front wheels. Therefore, it is important to fully analyze all the affecting factors of the system.

3.3.1 Ackerman

The Ackerman geometry was developed by Langensperger and Rudolf Ackerman in the 1880s and introduced a better way of turning a vehicle. Before this method, the tires was scrubbing and leaving marks when they turned because of the geometry making the front wheels to turn at an equal radius. This made it harder to turn as the inner wheel would slide sideways and forge unwanted wearing and heat.

The solution was to make a steering geometry to what is known as the Ackerman steering (fig. 4-7). When the vehicle is turning, the inner and outer wheels will travel at a different radius and different angle (miss-aligned); the inner wheel will travel at a smaller radius and a bigger angle than the outer wheel and hence, in a left turn i.e. the right wheel moves faster to undergo a larger distance in the same amount of time. It is important though to ensure that the wheels are traveling straight without any angle for full stability when not turning, and only are miss-aligned when cornering. Reverse-Ackermann is the geometry when the outside wheel turns at a greater angle than the inside wheel.

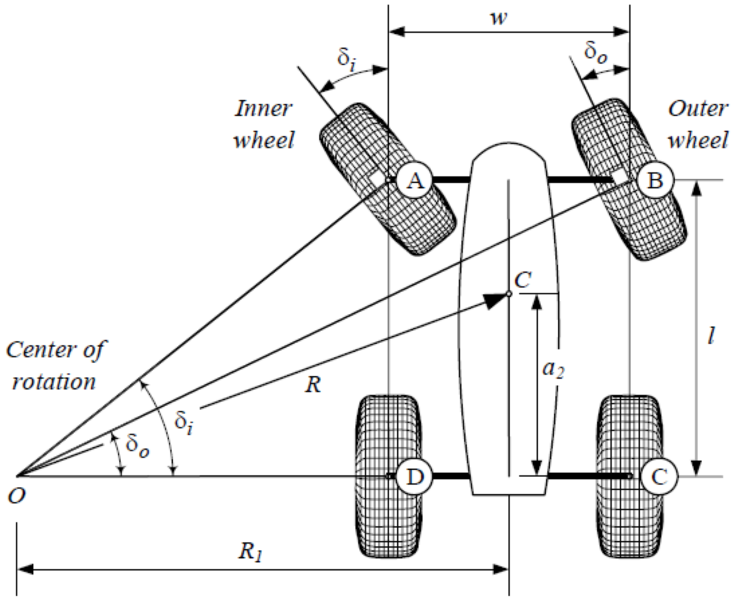

Figure 3-7: Ackermann Steering

The Ackerman condition is expressed by

$\cot\delta_o - \cot\delta_i = \frac{w}{l}$ (Equation 4.1)

where

$\delta_o: Steer\ angle\ of\ outer\ wheel\ with\ regard\ to\ center\ of\ rotation, O$

$\delta_i: Steer\ angle\ of\ inner\ wheel\ with\ regard\ to\ center\ of\ rotation, O$

$w: Track\ width\ at\ the\ front$

$l: Wheelbase\ (distance\ between\ the\ front\ and\ rear\ axle)$

It can be noted that the rear track has no effect of the Ackerman condition of a front-wheel steering vehicle and that the difference in the inner and outer steering angle will decrease as w/l decreases.

The angle for the inner and outer wheel can be expressed by

$\delta_i = \arctan(\frac{l}{R1-\frac{w}{2}})$ (Equation 4.2)

$\delta_o = \arctan(\frac{l}{R1+\frac{w}{2}})$ (Equation 4.3)

where

$R1: Radius\ from\ center\ of\ rotation\ to\ center\ of\ rear\ axle$

The radius to the mass center of the vehicle, of which the vehicle is turning, can now be found by simple Pythagoras equation:

$R^2 = {a_2}^2 + {R_1}^2$ (Equation 4.4)

where

$a_2: Distance\ from\ rear\ axle\ to\ the\ mass\ centre$

To produce Ackerman steering, the offset arm, in which the tie rod connects to the wheels, must be angled inwards with an angle β to create a change in the angle and unequal angular movement of the front wheels when turning (figure 4-8 and figure 4.9).

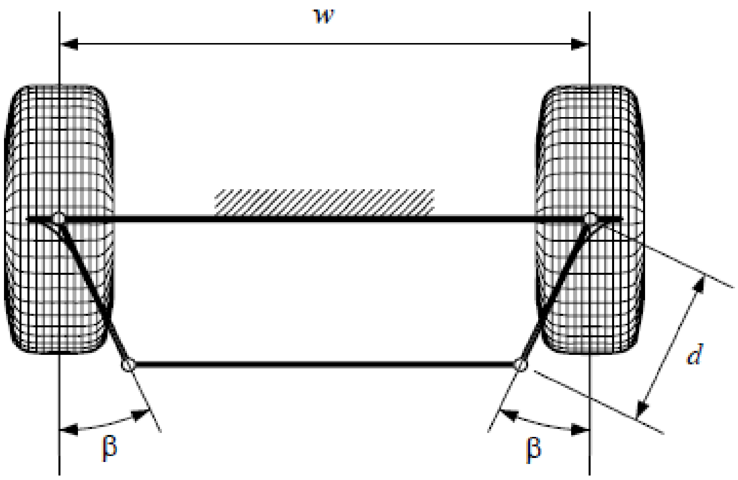

Figure 3-8: The vehicle is heading in a forward direction

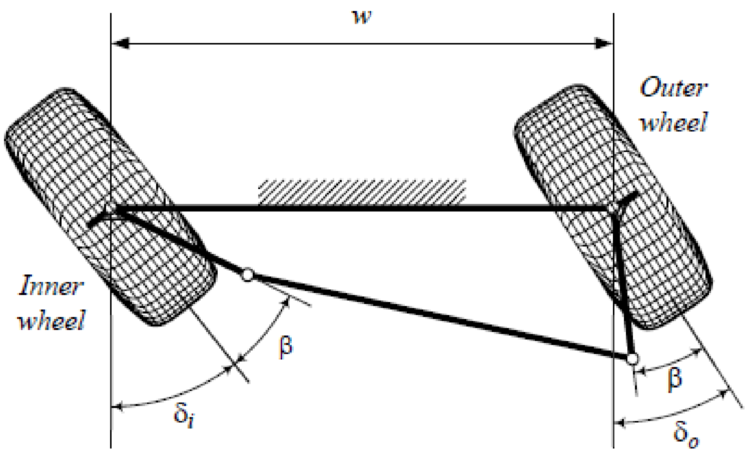

Figure 3-9: Ackermann steering gives different angles of the wheels during cornering

The angled offset arm can be expressed by terms of inner and outer wheel angle;

$$(w - 2d\sin\beta)^2 = (w - d\sin(\beta + \delta_i) - d\sin(\beta - \delta_o))^2 + (d\cos(\beta - \delta_o) - d\cos(\beta + \delta_i))^2$$
(Equation 4.5)

The figures above illustrate Ackermann geometry where the offset arm points rearward and the steering rack is placed behind the front axle. To obtain a reverse Ackermann geometry, the offset arm is pointed forward and the steering rack is placed in front of the forward axle.

Reversed Ackermann is often used in racing as the cars performance increases when cornering at high speeds. In a turn, the centrifugal forces will increase as the speed increases. This will also increase the slip angles as they are raising the lateral tire forces to prevent the car from sliding out. As the normal force is higher at the outer wheel in a turn due to weight distribution, a loss in friction coefficient will occur. This can be counterbalanced for by using a larger slip angle on the outer wheel which is obtained by reversed Ackermann geometry.

3.3.2 Toe In/Out

The toe in/out configuration explains the position of the wheels relative to the neutral toe position where the distance between the front parts of the wheels equals the distance between the rear parts, as seen in figure 4-10. The tie rods are adjusted to give the desired toe.

The toe configuration affects the handling of the vehicle and its performance on the straights and corners. Tire wearing will also be affected by the configuration chosen. By analyzing the race track, the best decision of the toe configuration can be made.

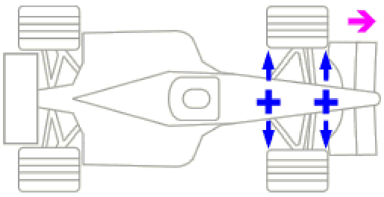

Figure 3-10: Neutral toe configuration

3.3.2.1 Toe In

In a “toe in” configuration, or positive toe, the front wheels are turned inwards giving a shorter distance between the front parts of the wheels and bigger distance at the rear parts as seen in figure 4-11.

By increasing the “toe in” configuration, better stability can be achieved on the straights, but it will give less turning response in the curves.

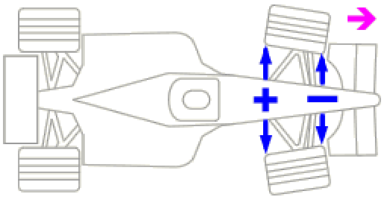

Figure 3-11: Toe in configuration

3.3.2.2 Toe Out

Figure 4-12 shows the “toe out” configuration where the distance at the front parts of the wheels are bigger compared to the rear parts. This is also called negative toe.

The “toe out” position is more common in racing as the wheels are aligned in a position that encourages the initiation of a turn.

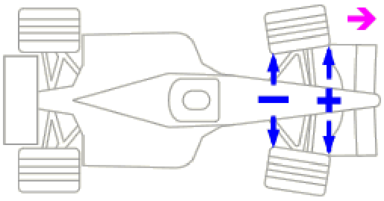

Figure 3-12: Toe out configuration

The “toe out” may appear in five forms at the vehicle:

- Static “toe out”
    - This is the “toe out” as a result of the adjustments of the tie rods. The tie rods are adjusted in a way that the wheels are “toed out”.

- “Toe out” due to the tie rods configuration
    - By using a shorter tie rod on the front left side compared to the front right side, the left wheel is steered at a larger angle than the right wheel when turning to the left. However, when turning to the right, this configuration will give a “toe in” position.

- Toe out on Ackerman steering
    - When using an Ackerman configuration, the “toe out” will occur when turning the wheels. This means that the toe out due to the Ackerman configuration only occurs in turns.

- Toe out due to bump steer
    - When riding, the ride motions and the body roll can lead to toe out

- Toe out due to slip angles
    - As the vehicle is turning, the outside contact patch between the wheel and the road will experience heavier load than the inside contact patch which result in a larger slip angle for the outside patch than the inside patch. As a result, the contact patches can be toed out.

3.3.3 Camber Angle

The camber angle is the angle between the vertical axis of the wheel and the vertical axis of the vehicle. The angle is negative if the wheel leans towards and positive if it leans away from the chassis.

The cornering forces on a wheel are dependable on the wheels angle on the road surface, and so the camber angle plays a major role on the forces acting on the car. It can also be used to increase the temperature in the wheels to their proper operating temperature by giving more negative camber angle.

3.3.4 Caster Angle

The caster angle is the angle between the pivot line and the vertical line at the center of the wheel. The angle adds damping to the steering system as it controls the steering; too much caster angle makes the steering heavy. The caster can be positive or negative:

- **Positive**: If the top pivot is placed further to the rear than the bottom pivot – axis tilted forward
- **Negative**: If the top pivot is placed further to the front than the bottom pivot – axis tilted backward

Positive caster angle enhance straight-line stability when driving forward as it straightens the wheels. This happens because the steering axis, which points forward, pulls the wheel along when the car moves.
As the caster angle is increased, camber gain can be achieved in corners.

3.3.5 Bump-steer

If the vehicle experience bumps on the track, the wheels may have the tendency to steer themselves without the driver doing any changes to the steering wheel. This is undesirable and known as bump-steer. The wheels will change between toe out and toe in as the suspension compress and de-compress during the bump. The steering wheel must be moved constantly to keep the vehicle in a constant turn. The wheel will also tend to toe out in a sharp turn as some of the weight is distributed to the outer wheel and hence makes the suspension on the outer wheel to compress.
Bump-steer will also cause increase tire wear

Bump-steer can be avoided by designing the same length and angle on the tie rod and the lover a-arm, and by ensuring that they both travel along the same arc during a bump.

By comparison; if the tie rod got a shorter length, the travelling arc would also be shorter. The shorter arc would pull on the wheel and make it toe in during a bump.

It can also be controlled by introducing shims on the connection point between the tie rod and the bolt, which will increase the elimination of the toe experienced. However, it is important that the size of the shims is within the limit of what the bolt can handle, as the shim introduces a moment to the bolt when the lateral force is acting on the tire. The bigger the lateral force, the smaller the shim should be to avoid big moment on the bolt.

3.3.6 Neutral-/under-/oversteer

A lot of factors are playing together when deciding how nicely a car will take a turn. The position of the center of gravity, the suspension geometry and the speed are all affecting the cornering ability. It can also change the cornering handling if the car is front wheel driven or rear wheel driven. By combining these factors, the car can experience what is known as neutral-, under- or oversteer.

The terms understeer and oversteer is relative to the geometric path established by the Ackermann steering angle;

$$\delta = \frac{l}{R} \qquad \text{(Equation 4.6)}$$

3.3.6.1 Neutral steer

If the center of gravity of the vehicle is positioned at the middle of the wheelbase with length l, the front and rear cornering stiffness is equal;
$a = b = l/2$ and $C_F = C_R$

The cornering forces of the front and rear tires are reacting the centrifugal force pulling the vehicle sideways. The force equilibrium is

$$Centrifugal\ force = C_F * \alpha_F + C_R * \alpha_R \qquad \text{(Equation 4.7)}$$

The moment equilibrium is

$$C_F * \alpha_F * a = C_R * \alpha_R * b \qquad \text{(Equation 4.8)}$$

With the assumption that $a = b = l/2$:
$\Rightarrow \alpha_F = \alpha_R$

Neutral steer is obtained if the vehicle follows the geometric path established by the Ackermann steering angle as lateral acceleration A_Y is applied. Since $C_F = C_R = C$ and $\alpha_F = \alpha_R = \alpha_1$

$$W * A_Y = 2C\alpha_1$$

3.3.6.2 Understeer

By moving the center of gravity ahead of the center of the wheelbase, the static load on the front wheels increases.
By assuming the location of the center of gravity at a distance 1/3 behind the front track implies that

the front wheels are carrying twice the load of the rear; 2/3 W on the front wheels and 1/3 W on the rear wheels. As the side forces are reacted in the turn, the front track takes 2/3 of the cornering force and the rear 1/3.

At the rear:

$$WA_Y = C(\alpha_F + \alpha_R) = C(2\alpha_R + \alpha_R) = 3C\alpha_R = 2C\alpha_1$$

$$\Rightarrow \alpha_R = \frac{2}{3}\alpha_1$$

The rear slip angle α_R gets a 1/3 reduction due to rotation effect and this must be compensated for by an increase in the steer angle δ. α_R will try to steer the car into the turn.

At the front:

$$WA_Y = C(\alpha_F + \alpha_R) = C\left(\alpha_F + \frac{1}{2}\alpha_F\right) = C\frac{3}{2}\alpha_F = 2C\alpha_1$$

$$\Rightarrow \alpha_F = \frac{4}{3}\alpha_1$$

To bring the front slip angle to 4/3 α_1, another 1/3 α_1 is needed and is obtained by an increase in the steer angle δ. α_F will try to steer the car out of the turn.

The net steering effect is

$$\alpha_F - \alpha_R = \frac{4}{3}\alpha_1 - \frac{2}{3}\alpha_1 = \frac{2}{3}\alpha_1$$

out of the turn as the front track predominates. It is required 2/3 α_1 more than for the neutral steer car to obtain the specified radius.

The total steering angle is

$$\delta = \frac{l}{R} + (-\alpha_F + \alpha_R) = \frac{l}{R} - \frac{2}{3}\propto_1$$

More steer angle is required to hold the radius of the turn.

3.3.6.3 Oversteer

If the center of gravity is moved 2/3 behind the front axle, the static load is 2/3 on the rear wheels and 1/3 on the front wheels. As the side forces are reacted in the turn, the front track takes 1/3 of the cornering force and the rear 2/3.

At the rear:

$$WA_Y = C(\alpha_F + \alpha_R) = C\left(\frac{1}{2}\alpha_R + \alpha_R\right) = C\frac{3}{2}\alpha_R = 2C\alpha_1$$

$$\Rightarrow \alpha_R = \frac{4}{3}\alpha_1$$

The rear slip angle gets an increase due to tail swing effect and predominates in the turn.

At the front:

$$WA_Y = C(\alpha_F + \alpha_R) = C(\alpha_F + 2\alpha_F) = 3C\alpha_F = 2C\alpha_1$$

$$\Rightarrow \alpha_F = \frac{2}{3}\alpha_1$$

The net steering effect is

$$\alpha_F - \alpha_R = \frac{2}{3}\alpha_1 - \frac{4}{3}\alpha_1 = -\frac{2}{3}\alpha_1$$

into the turn as the rear track predominates. It is required 2/3 α_1 less than for the neutral steer car to obtain the specified radius.

The total steering angle is

$$\delta = \frac{l}{R} + (-\alpha_F + \alpha_R) = \frac{l}{R} + \frac{2}{3}\propto_1$$

Less steer angle is required to hold the radius of the turn.

4 STEERING SYSTEM DESIGN GUIDELINES

4.1 Formula Student SAE 2013 Rules

The rules for Formula Student 2012 are valid for the competition at Silverstone in July 2013. In addition, some minor changes have been made and are pointed in an overview for 2013. The rules can be found in appendix C.

4.1.1 Wheels

- The wheels of the car must be 203.2 mm (8.0 inches) or more in diameter. (SAE 2012)
- Any wheel mounting system that uses a single retaining nut, must incorporate a device to retain the nut and the wheel in the event that the nut loosens. (SAE 2012)
- Teams using modified lug bolts or custom designs will be required to provide proof that good engineering practices have been followed in their design. (SAE 2012)

New rule by 2013:

- Extended or composite wheel studs are prohibited. (SAE 2013)

4.1.2 Tires

- Vehicles may have to types of tires:
  - Dry tires:
    The dry tires may be any size or type. They may be slicks or treaded. (SAE 2012)
  - Rain tires:
    The rain tiers may be any size or type. They may be threaded or grooved.
    The tread pattern or grooves must have been molded by the tire manufacturer or were cut by the tire manufacturer. (SAE 2012)
    There must be a minimum tread depth of 2.4 mm (3/32 inch). (SAE 2012)

New rule by 2013:

- Remoulded or re-treaded tires are prohibited. (SAE 2013)

4.1.3 Steering

- The steering wheel must be mechanically connected to the wheels, i.e. “steer-by-wire” is prohibited or electrical actuated steering is prohibited. (SAE 2012)
- The steering system must have positive steering stops that prevent the steering linkages from locking up. The stops may be placed on the uprights or on the rack and must prevent the tires from contacting suspension, body, or frame members during the track event. (SAE 2012)
- Allowable steering system free play is limited to seven degrees (7^0) total measured at the steering wheel. (SAE 2012)

- A free vertical cross section, which allows the template to be passed horizontally through the cockpit to a point 100 mm rearwards of the face of the rearmost pedal when in the inoperative position, must be maintained over its entire length. (SAE 2012)

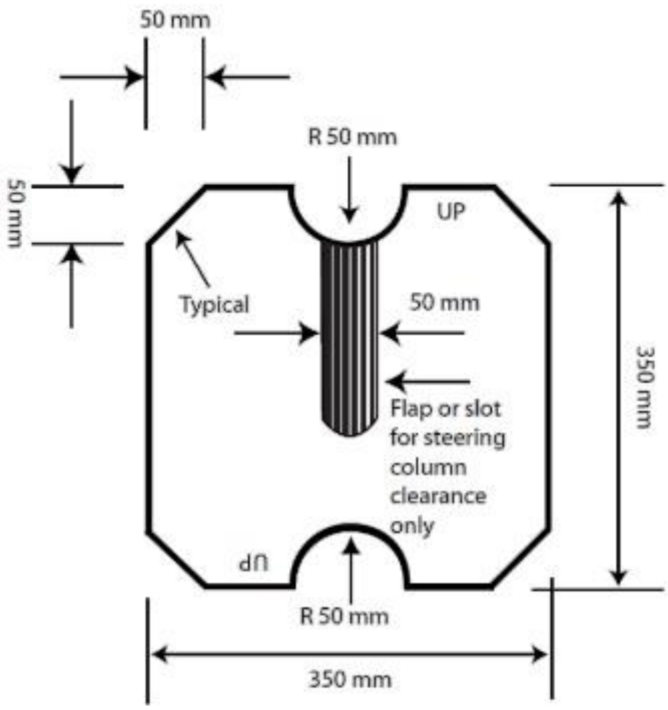

Figure 4-1: Cockpit template, Formula SAE

4.1.4 Steering Wheel

- The steering wheel must be attached to the column with a quick disconnect. (SAE 2013)
- The steering wheel must have a continuous perimeter that is near circular or near oval. “H”, “figure 8” or cutout wheels are not allowed. (SAE 2013)
- In any angular position, the top of the steering wheel must be no higher than the top-most surface of the Front Hoop. (SAE 2013)

5 STEERING SYSTEM DESIGN

5.1 Steering System Considerations

When designing the steering system, some factors have been considered, and the performance of the last year's formula student car has been analyzed;

- *Power assisted or manual assisted steering system*!
  By comparing the new race car design (body, frame, engine etc.) with the last year's design, the weight is calculated to be less than the 256 kg of last year (2012). The weight of the frame will be the same as last year, but using less material-thickness on the body, and lighter battery and radiator, the new weight will be approximately 240 kg. With addition with the driver, at a maximum weight of 80 kg, the total weight will be 320 kg.

  The weight of the race car is small, compared to other commercial vehicles, which makes it easy to turn at low speeds. It will also be operated in races and needs a fast and reliable steering system. The rack and pinion steering gear is the best option for this car.

  By comparing manual and power assisted steering, the power assisted steering option is not preferable due to different factors: more weight would be put on the car with a power assisted steering system, due to different factors:
    - More weight will be put on the racing car with more components as the hydraulic pump, valves and hoses.
    - The risk of leakage and spill, and even fire, will rise with a hydraulic pump, flow control valves and hoses. This is not preferable in racing conditions with hot engines and high speeds.
    - With the option of electrical driven system, a bigger battery will be needed which raises the total weight. An electrical system is also at bigger risk when it comes to errors due to rain and technical faults.

  Taking these factors into consideration, a manual steering rack and pinion gear system is chosen with a linear steering rack.

- *The drivers of last year's team (2012) were reporting that the vehicle was easy to operate and it turned easily in the corners. However, the vehicle had problems with driving straight forward without turning to one of the sides.* The steering wheel was also too wobbling.
  This is coped with by analyzing the steering system in MSC ADMAS to get a visualization of the handling of the vehicle.
  The steering wheel was stabilized with ball bearings.

- *The weight distribution of the last year's car was too far to the front.*
  To get a better weight distribution to the rear of the vehicle, the a-arms supporting the front wheels have been redesigned placing the wheels more ahead compared to the last year's position. This was done by analyzes in the other master thesis. The lower a-arms are pointing more ahead than the upper a-arms, making a caster angle on the front wheels. This has resulted in a new position of the steering rack further to the front to avoid big angles and big momentum on the tie rods.

Placing the weight distribution more to the rear will also give better performance with the manual steering rack.

- *Last year (2012), the team were choosing dry and wet Hoosier 20,5 x 7,0 – 13 C2500 racing tires. The feedback was positive and both types of tires were used during the competition as there was raining some of the days. Hoosier is also a popular brand used by other teams during Formula Student.*
  Because of the positive feedback from last year, and budget considerations, it was decided to continue to use the Hoosier racing tires that were bought in last year. Some teams are using 10 inches wheels as this will lower the total weight. However, the 13 inches wheels give a wider contact patch between the tire and the road compared with the 10 inches wheels, which is preferable for a racing car. Also, the budget did not allow us to change wheels this year.

  Hoosier is suited for small Formula Student cars and has been used by other winner teams, as stated on their homepage:
  "Global formula racing wins 3RD consecutive FSAE title on Hoosiers" (www.hoosiertire.com).

- As there will be new positions of the front a-arms, there will also be manufactured new uprights. As a result, the tie rods and steering rack can be placed in a new and better position to avoid big tie rods momentum forces. The offset arm will be designed for optimal forces and reversed-Ackermann.

- The same steering wheel w/ paddle shifters as last year will be disassembled, and assembled on the new car.

- The steering system will be designed for reversed Ackermann steering giving optimal handling in the skid-pad event. The skid-pad layout consists of two concentric circles with an inner diameter of 15.25 meters and a horizontal distance of 3 meters between the cones.

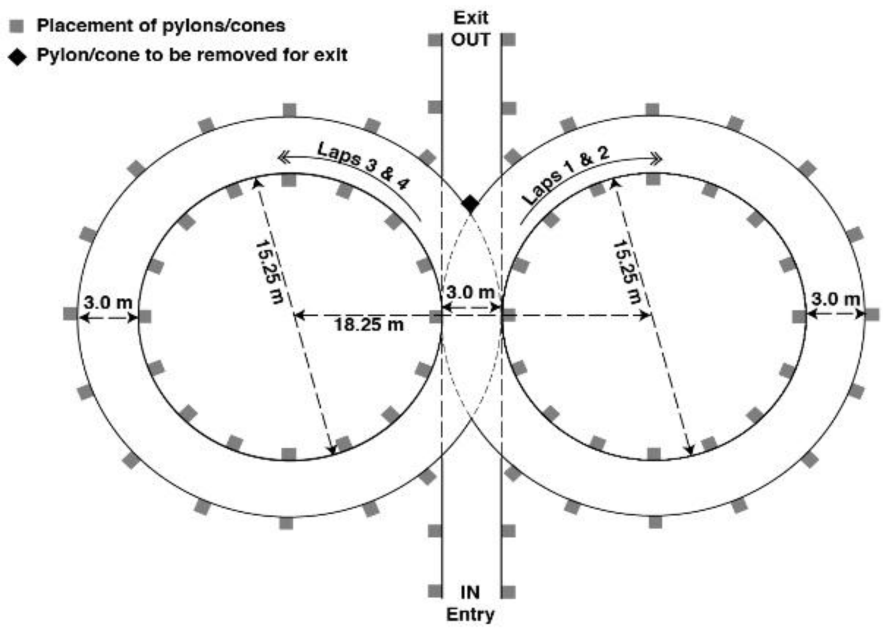

Figure 5-1: Skid-pad layout

5.2 The Seering System

The steering system consists of a steering wheel with paddle shifters mounted on a quick release mechanism. The quick release is connected to a double linkage steering column which is connected to the steering rack. A tie rod with a rod end in each end is connected to the steering rack at one end, and to the offset arm at the other end (figure 6-2).

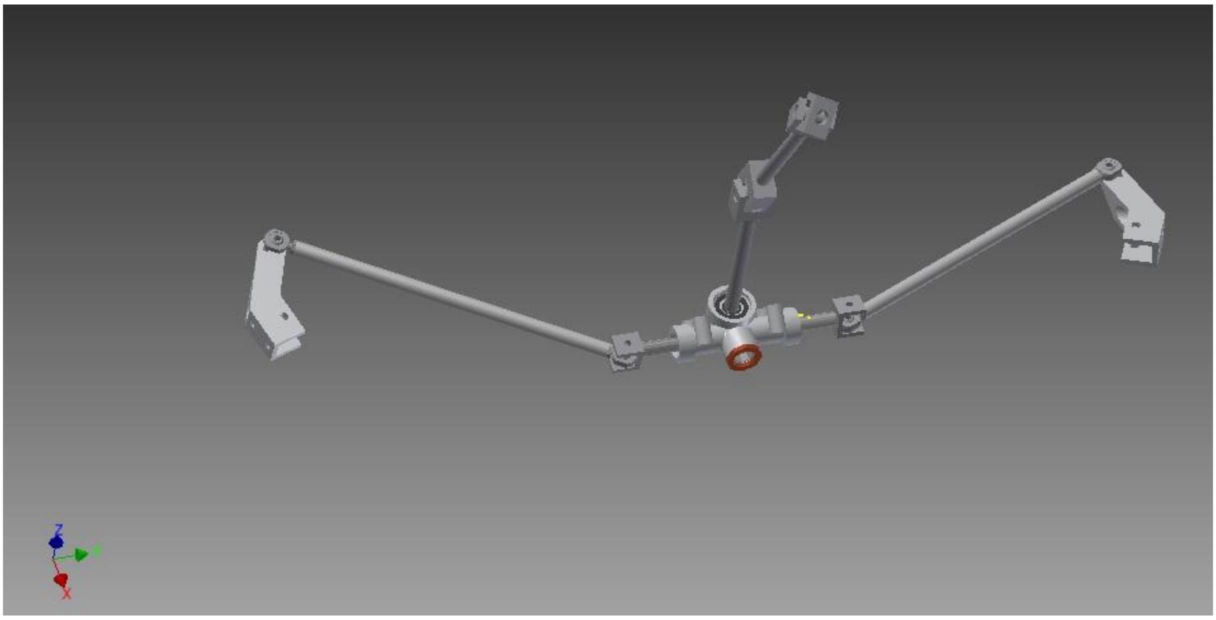

Figure 5-2: Steering system without steering wheel and quick release mechanism

5.3 The Acting Forces

To be able to design the tie rods for the forces transferred from the front tires via the rod ends, a calculation of the tire forces has been done. The forces are depending on the slip angles forced on the tire VS the cornering force.

The manufacturer is not obligated to publish these results, but some do publish them. For the Hoosier tires, the test results are not published and not given when buying the tires. However, Milliken Research Associates is a tire test consortium of Formula SAE teams who volunteers to test and obtain tire data. Any results obtained within the consortium are not allowed to be published on the internet, as stated by the rules: "Individuals and teams are prohibited from donating or selling the data to any other individual, group, team or university, or posting it on the internet " (Millikenresearch). These test results can be obtained by paying a registering fee of 500 USD. As the 2013 budget are strict, this is not a possibility.

A former Master Thesis in 2006 at the Technical University of Eindhoven (A. van Berkum)has obtained test results for Avon 7.0/20.0 – 13 pro series tires. As we are using Hoosier 7.0/20.5 – 13 racing tires, the dimensions of the tires are almost identical as we only got 0,5 inches more at the outer dimension of the tire. Hence, the results for the Avon tire was used in further calculations to get an estimate of the forces acting on the Hoosier tires.

Figure 6-3 shows the slip angle vs. cornering force, tested with slip angles from -7 to 7 degrees.

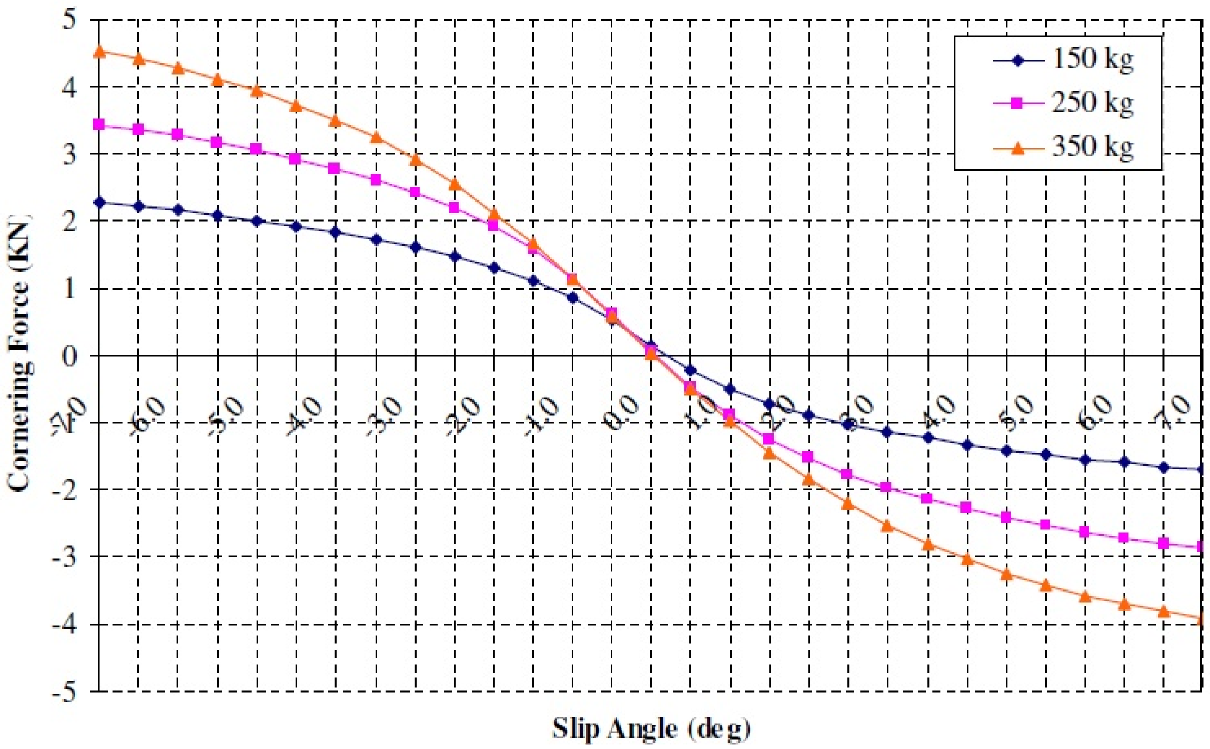

Figure 5-3: Slip angle VS cornering force for Avon 7,0/20,0 – 13pro-series

The test results have been obtained with normal forces of 1500 N, 2500 N and 3500 N (approx. 150 kg, 250 kg and 350 kg). It is clearly showed that the cornering force is increased with bigger normal forces on the tire and at bigger slip angles. The total weight of the vehicle should be reduced as much as possible to avoid big cornering forces.

The forces that are acting on the racing car during the race will be down-forces, bump forces, cornering forces, accelerating and braking forces.

The forces are calculated with a total weight of 320 kg including the driver. Further, a weight distribution of 50/50 front and rear are assumed. In table 6-1, the weight distributed on the tires is shown.

Table 6-1: The weight distribution on the car on the rear and front wheels

Tire	Weight [kg]	Force [N]	% of total
Left/Right front	80	784.8	25
Both front	160	1569.6	50
Left/Right rear	80	784.8	25
Both rear	160	1569.6	50

When calculating the cornering forces it is assumed that the maximum cornering forces are obtained. This will happen at a small negative camber angle, typically around – ½ degrees. This is due to the contribution of camber trust which will add an additional lateral force due to elastic deformation [Hagerman. John, Grassroots Motorsports Magazine].

5.3.1 Down-Forces

When using a front and back wing on the race car, the aerodynamic forces will increase and produce a down-force on the front and rear tires. This force is known as aerodynamic grip force and will press the race car against the surface of the race track.

The created down-force is dependent on the shape and the angle of attack. With a larger surface area a greater down-force are created. It will also increase when cornering.

The formula for the down-force created by a wing is given as:

$$D = \frac{1}{2}\,(Wingspan * Height * Angle\ of\ attack) * F * \rho * v^2 \qquad \text{(Equation 6.1)}$$

where
F = lift coefficient
ρ = air density in kg/m^2
v = velocity in m/s

The down-force equals v^2 and will increase or decrease linearly with a change in the speed. At 75 km/h the down-force is 1040 N at the front wheels together (dukemotorsports).

As the force changes linearly, the rate of change can be calculated:

$$k * v^2 = 1040\,N \qquad \text{(Equation 6.2)}$$

$$k * (75\frac{km}{h})^2 = 1040\,N$$

$$k = 0{,}1848\,\frac{N}{(\frac{km}{h})^2}$$

When designing the steering system for the down-force, the force generated by the rear and front wing at a speed of 110 km/h has been calculated. The velocity is used to calculate a bigger force than will probably occur during the race as the race car would probably not reach a speed of 110 km/h. A safe margin is needed to assure that the system can cope with the exerted force.

At a speed of 140 km/h, the down-force is;

$$Down\,force = k * v^2 = 0.1848\ \frac{N}{\left(\frac{km}{h}\right)^2} * \left(110\ \frac{km}{h}\right)^2 = 2236.08\,N\ \approx 2236.1\,N$$

By assuming that this down-force is distributed by the front and rear wing and it is distributed 50/50 front and rear, table 6.2 shows the distribution of the down-force on the wheels.

Table 6.2: Down-force distribution by the rear and front wing at 110 km/h

	Down force [N]
Front left and right wheel	559
Front wheels	1118
Rear left and right wheel	559
Rear wheels	1118

This equals a down-force of 0.7 G.

5.3.2 Bump Forces

Bump force are the amount of force applied on the car when driving over a bump. The force depends on both speed and if there exist any aerodynamic forces due to the usage of wings which will increase the bump forces.

An assumption of 3,5 G has been used when calculating the forces.

Table 6.3: Bump forces acting on the wheels

	Bump force [N]
Rear wheels	5665
Front wheels	5665

5.3.3 Cornering Forces

During cornering the tires produce lateral forces. The lateral forces act on the car's mass and as a result the car will turn. On a left turn, the weight distribution on the front tires will increase on the outer tire and decrease on the inner tire as a result of the car "leaning" to the right.

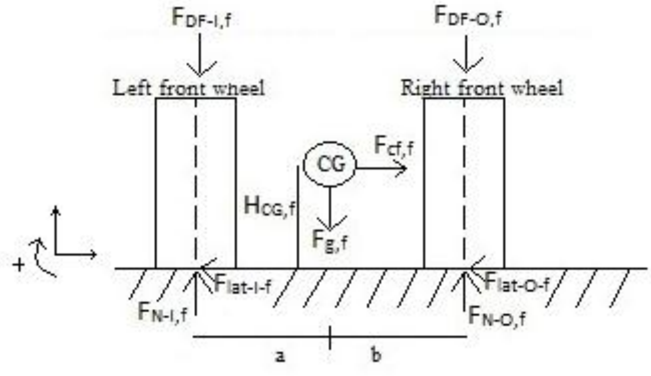

Figure 5-4: Cornering forces on inner and outer front wheel

where

$H_{CG,f}$	Height of center of gravity at front
$F_{cf,f}$	Centrifugal force at front
$F_{DF-I,f}$	Down-force at inner tire at front
$F_{DF-O,f}$	Down-force at outer tire at front
$F_{N-I,f}$	Normal force at inner tire at front
$F_{N-O,f}$	Normal force at outer tire at front
$F_{lat-I,f}$	Lateral force at inner tire at front
$F_{lat-O,f}$	Lateral force at outer tire at front
$F_{g,f}$	Gravity force at front

The distance

$a + b = Front\ track\ width$

where

Front track width = 1290 mm

a = b = 645 mm

$H_{CG,f,r}$ = 340mm

The equilibrium of momentum around CG:

$$\sum M_{CG,f} = 0 \qquad \text{(Equation 6.3)}$$

$$F_{N-I,f} * a + F_{lat-I,f} * h_{CG,f} + F_{lat-O,f} * h_{CG,f} + F_{DF-O,f} * b - F_{DF-I,f} * a - F_{N-O,f} * b$$

The equilibrium in vertical direction:

$$\sum F_y = 0 \qquad \text{(Equation 6.4)}$$

$$F_{N-I,f} + F_{N-O,f} - F_{DF-I,f} - F_{DF-O,f} - F_{g,f} = 0$$

The forces $F_{lat-I,f}$ and $F_{lat-O,f}$ can be written as functions of $F_{N-I,f}$ and $F_{N-O,f}$ using the standard friction model:

$$F = \mu * F_N \qquad \text{(Equation 6.5)}$$

$F_{lat-I,f} = \mu_{lat,f} * F_{N-I,f}$ (Equation 6.6)

$F_{lat-O,f} = \mu_{lat,f} * F_{N-O,f}$ (Equation 6.7)

The same equations can be used for the forces on the rear tires. The friction coefficient is assumed to be 0,5 times smaller on wet road.
Figure 6-5 and figure 6-6 shows the linear approximation of μ_{lat} on dry and wet road for the front and rear tire.

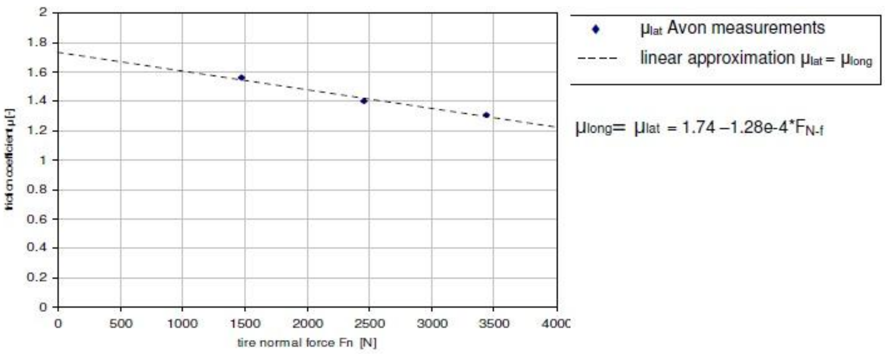

Figure 5-5: $\mu_{lat,f}$ on dry road for front and rear tire

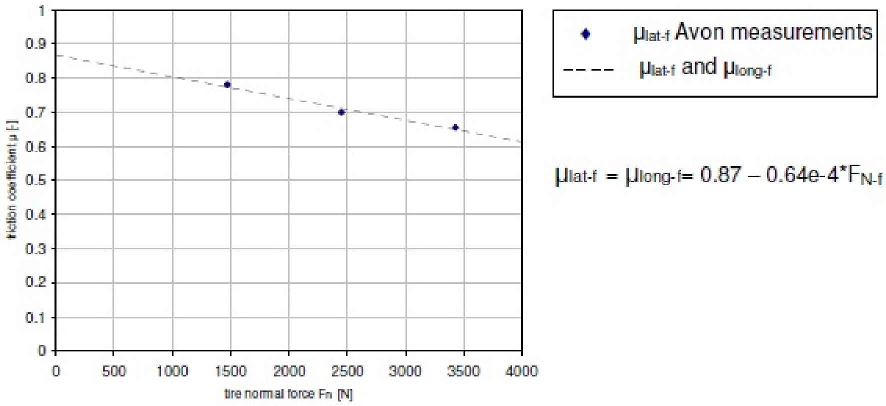

Figure 5-6: $\mu_{at,f}$ on wet road for front and rear tire

The normal force will equal the gravity force and down-force. Table 6.4 shows the normal forces acting on the tires.

Table 6.4: Normal force at front and rear tires

	Normal force [N]
Front left and right tire	1343.8
Front tires	2687.6
Rear left and right tire	1343.8
Rear tires	2687.6

When cornering, an amount of weight will be increased to the outer wheel and the same amount will be decreased at the inner wheel as the car is “leaning”.

The amount that is increased and decreased in F_n on dry road at the front and rear tire is calculated below with a µ-value of 1,58. The same calculation can be done on a wet road with a µ-value of 0,79. The friction coefficient is based on a normal force of 1343.8 N (784.8 N at front tire + 559 N down-force at front tire) and can be seen in appendix F.

$G_{lat} = (1 + 0.7)G * \mu_{lat}$ (Equation 6.8)

$G_{lat} = 1.7 * 9.81\frac{m}{s^2} * 1,58 = 26.35\frac{m}{s^2}$

$F = G_{lat} * M_{car,f,r}$ (Equation 6.9)

$M_{car,f,r} = Weight\ of\ car\ at\ front\ tires$

$F = 26.35\frac{m}{s^2} * 160\ kg = 4216\ N$

The outer front wheel will get an increase in F_N;

$F_{N-o,f} = \frac{F*H_{CG,f,r}}{Track\ width}$ (Equation 6.10)

$H_{CG,f,r} = Height\ of\ center\ of\ gravity\ at\ front\ and\ rear = 340\ mm$

$Front\ track\ width = 1290\ mm$

$F_{N-o,f} = \frac{4216\ N*340mm}{1290mm} = 1111.19\ N\ \approx 1111.2\ N$

The inner front wheel will get a decrease in F_N by the same amount.

When calculating for the rear, a track width of 1240 mm is used as the car is narrower at the rear track.

The increase and decrease in F_N at the rear is

$F_{N-o,r} = \frac{F*H_{CG,f,r}}{Rear\ track\ width}$

$F_{N-o,r} = \frac{4216\ N*340mm}{1240mm} = 1156.0\ N$

The cornering forces are presented in table 6.5 below.

Table 6.5: Cornering forces at front and rear wheels

	Dry road cornering forces [N]	**Wet road cornering forces [N]**
$\mathbf{F_{N-I,f}}$	232.6	788.2
$\mathbf{F_{N-O,f}}$	2455.0	1899.4
$\mathbf{F_{lat-I,f}}$	367.5	622.7
$\mathbf{F_{lat-O,f}}$	**3878.9**	1500.5
$\mathbf{F_{cf,f}}$	4246.4	2123.2
$\mathbf{F_{DF-I,f}}$	906.0	906.0
$\mathbf{F_{DF-O,f}}$	906.0	906.0
$\mathbf{F_{N-I,r}}$	187.8	765.8
$\mathbf{F_{N-O,r}}$	2499.8	1921.8
$\mathbf{F_{lat-I,r}}$	296.7	605.0
$\mathbf{F_{lat-O,r}}$	3949.7	1518.2
$\mathbf{F_{cf,r}}$	4246.4	2123.2
$\mathbf{F_{DF-I,r}}$	906.0	906.0

$F_{DF\text{-}Orf}$	906.0	906.0

The biggest lateral force on the front tire is 3878.9 N and will occur at the outer tire on a dry road. The tie rods and bolts must be designed to resist this lateral load.

5.3.4 Braking Forces

The mass distribution will change during the braking sequence; more mass will be distributed to the front tires from the rear tires. During braking, all tires will produce friction forces. Figure 6-7 shows the forces that appear during braking.

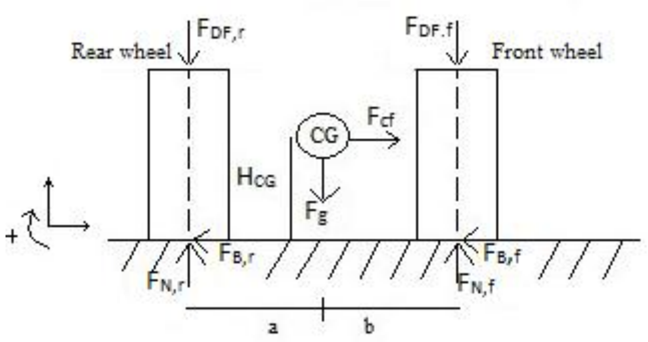

Figure 5-7: Braking forces at front and rear tire

Where

$F_{N,r}$ Normal force at rear tire
$F_{N,f}$ Normal force at front tire
$F_{B,r}$ Braking force at rear tire
$F_{B,f}$ Braking force at front tire
$F_{DF,r}$ Down-force at rear tire
$F_{DF,f}$ Down-force at front tire
F_g Gravity force
F_{cf} Centrifugal force

The distances are
a = 800 mm
b = 800 mm
h_{CG} = 340 mm

The equilibrium of momentum around CG:

$$\sum M_{CG} = 0 \qquad \text{(Equation 6.11)}$$
$$F_{N,r} * a + F_{B,r} * h_{CG} + F_{B,f} * h_{CG} + F_{DF,f} * b - F_{DF,r} * a - F_{N,f} * b$$

The equilibrium in vertical direction:

$$\sum F_y = 0 \qquad \text{(Equation 6.12)}$$
$$F_{N,r} + F_{N,f} - F_{DF,r} - F_{DF,f} - F_g = 0$$

The forces $F_{B,r}$ and $F_{B,f}$ can be written as functions of $F_{N,,r}$ and $F_{N,,f}$ using equation 6.5:

$F_{B,r} = \mu_{long,r} * F_{N,r}$ (Equation 6.13)

$F_{B,f} = \mu_{long,f} * F_{N,f}$ (Equation 6.14)

An equal amount of F_N will increase and decrease during the braking; More mass will move to the front as the same amount will move away from the rear. Below is the amount calculated with the same procedure as in the cornering forces, but now the track width is substituted with the length of the wheelbase.

$G_{long} = (1 + 0.7)G * \mu$ (Equation 6.15)

$G_{long} = 1.7 * 9.81 \frac{m}{s^2} * 1{,}58 = 26.35 \frac{m}{s^2}$

$F = G_{long} * M_{car,f,r}$ (Equation 6.16)

$M_{car,f,r} = 160$ kg

$F = 26.35 \frac{m}{s^2} * 160kg = 4216.0\ N$

The front wheel will get an increase in F_N;

$F_{N,increse} = \frac{F * H_{CG,f,r}}{Length\ center\ rear\ to\ center\ front\ tire}$ (Equation 6.17)

$F_{N,increase} = \frac{4216\ N * 340mm}{1600\ mm} = 895.9\ N$

The F_N at the rear wheel will be decreased by the same amount.

When calculating the braking forces a simplification has been done. The normal force used is 1569.6 N (the total weight on one side of the vehicle without down-force). The down-force has not been taken into consideration for simplification reasons, as it will have a high value when braking from high speeds, and decrease as the speed decreases. The result in table 6.6 should therefore be seen as a guidance of the braking forces.

The values for wet road braking has been calculated with μ=0.79.

Table 6.6: Braking forces on rear and front wheel on dry and wet road

	Braking forces on dry road [N]	**Braking forces on wet road [N]**
$F_{N,r}$	673.7	1121.6
$F_{N,f}$	2465.5	2017.0
$F_{B,r}$	1064.4	886.1
$F_{B,f}$	3895.5	1593.4
F_{cf}	4959.9	2479.5

5.4 The Design

It is important to design a safe and reliable steering system to avoid breakdowns due to big forces and momentums in the components due to poor design and misplacements. Ackermann and bump steer considerations are important to avoid tire tearing, unstable turning, and good performance of the car as well as to make an optimal offset arm connected to the upright. The offset arm decides the angle for the tie rod and may in some cases produce big momentum and forces if the angle is too big.
The position of the steering rack can decrease the forces if the right position is chosen.

5.4.1 The Offset Arm

The offset arm is the connection between the tie rod and the upright on each front wheel. When the tie rod changes position it pushes or pulls on the offset arm, changing the angle of the wheel and the car is turning. The geometry of the offset arm is therefore important as it controls how much the wheel turns and hence the angle of the wheel.

Rapid prototyping was used in the designing process as the offset arm was printed in a 3D-printer to visualize the part and its position on the wheel.

The offset arm was designed for reversed Ackermann steering geometry pointing forward on the upright and the steering rack placed in front of the front axle (see drawings in Appendix F). It was designed for maximum performance of the car on the skid-pad event allowing high speed when cornering. The event consists of two pairs of concentric circles making an eight pattern figure (section 6.1). The diameter of the inner circle is 15.25 meters (radius of 7.625 meters).

Equation 4.4 gives the radius from the center of rotation to the center of the rear axle:

$$R_1 = \sqrt{(800\ mm)^2 + (7625\ mm)^2} = 7582.9\ mm$$

The inner and outer wheel angle can then be found by equation 4.2 and 4.3:

$$\delta_o = \arctan\left(\frac{l}{R1-\frac{w}{2}}\right) = \arctan\left(\frac{1600\ mm}{7582.9\ mm-\frac{1290\ mm}{2}}\right) = 12.98\ degrees \approx 13.0\ degrees$$

$$\delta_i = \arctan\left(\frac{l}{R1+\frac{w}{2}}\right) = \arctan\left(\frac{1600\ mm}{7582.9\ mm+\frac{1290\ mm}{2}}\right) = 11.0\ degrees$$

The angle of the offset arm can now be found by equation 4.5. The arm has a horizontal length of 90 mm from the center of the tire towards the rim.

$$(1290mm - 2 * 90.0mm * \sin(\beta\ degrees))^2 = (1290mm - 90.0mm * \sin(\beta\ degrees + 12.98\ degrees) - 90.0mm * \sin(\beta\ degrees - 11.0\ degrees))^2 + (90.0mm * \cos(\beta\ degrees - 11.0\ degrees) - 90.0\ mm * \cos(\beta\ degrees + 12.98\ degrees))^2 \rightarrow \beta = 39.3\ degrees$$

The design will allow the steering rack to move 30 mm to the left or to the right during a cornering process before the offset arm comes into contact with the lower a-arm. Before the movement, the angle of the arm is 39.3 degrees relative to the straight forward direction. With a horizontal length of 100 mm, the y-component is

$$\sin(39.3\ degrees) = \frac{y\ mm}{100\ mm}$$

⇒ y component = 63.34 mm

After a 30 mm movement, the y component is

$$63.34\ mm + 30\ mm = 93.34\ mm$$

and the angle of the arm is

$$\sin(x\ degrees) = \frac{93.34\ mm}{100\ mm} = \ 68.97\ degrees$$

relative to the straight forward direction.

The difference in the angle, and hence the highest possible steering angle for the wheels, is

$$68.97\ degrees - 39.30\ degrees = 29.67\ degrees$$

and will occur at the outer wheel due to the reversed Ackermann geometry. This corresponds to a turn with a radius of

$$\tan(29.67\ degrees) = \frac{1600\ mm}{R1 - \frac{1290}{2}}$$

⇒ R1 = 3453.51 mm

$$R = \sqrt{800.00\ mm^2 + 3453.51\ mm^2} = 3544.96\ mm = 3545\ mm$$

The inner wheel angle is

$$\delta_i = \arctan\left(\frac{l}{R1 + \frac{w}{2}}\right) = \arctan\left(\frac{1600\ mm}{3453.51\ mm + \frac{1290\ mm}{2}}\right) = 21.325\ degrees = 21.33\ degrees$$

5.4.2 Steering Rack Position

The steering rack will be placed within the marked area of the frame (see Appendix G).

The mechanical and pneumatic trail will affect the position of where the resultant lateral force will work on the contact patch, and hence the decisions of the placement of the steering rack to try to decrease the working forces.

The caster angle controls the mechanical trail and can be seen in figure 6-8.

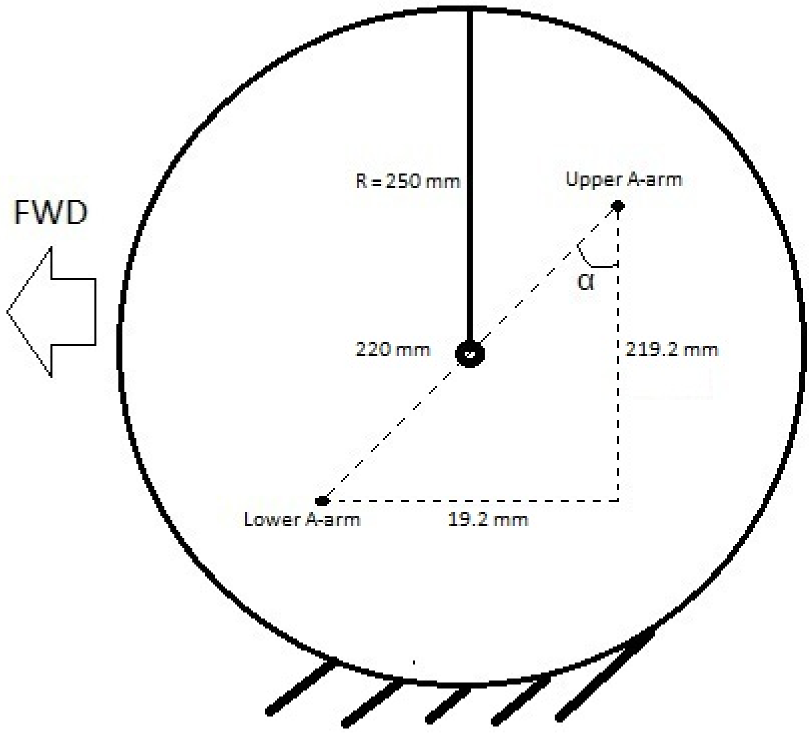

Figure 5-8: The caster angle, α

The caster angle is
$\alpha = \operatorname{atan}\left(\frac{19.2}{219.2}\right) = 5.0\ degrees$

This gives a mechanical trail of (Equation 3.2)

$$Mechanical\ trail = \tan(5\ degrees) * \ 250\ mm = 21.87\ mm = 21.9\ mm$$

It is of interest to know at which slip angle the maximum lateral force occurs and the corresponding self-aligning torque at this slip angle as the pneumatic trail can then be found. This has been done by quadratic spline interpolation:

$$\alpha(F_Y) = \frac{(F_Y-F_{Y2})*(F_Y-F_{Y3})}{(F_{Y1}-F_{Y2})*(F_{Y1}-F_{Y3})} * \alpha_1 + \frac{(F_Y-F_{Y1})*(F_Y-F_{Y3})}{(F_{Y2}-F_{Y1})*(F_{Y2}-F_{Y3})} * \alpha_2 + \frac{(F_Y-F_{Y1})*(F_Y-F_{Y2})}{(F_{Y3}-F_{Y1})*(F_{Y3}-F_{Y2})} * \alpha_3$$

(Equation 6.18)

$$M_Z(\alpha) = \frac{(\alpha-\alpha_2)*(\alpha-\alpha_3)}{(\alpha_1-\alpha_2)*(\alpha_1-\alpha_3)} * M_{Z1} + \frac{(\alpha-\alpha_1)*(\alpha-\alpha_3)}{(\alpha_2-\alpha_1)*(\alpha_2-\alpha_3)} * M_{Z2} + \frac{(\alpha-\alpha_1)*(\alpha-\alpha_2)}{(\alpha_3-\alpha_1)*(\alpha_3-\alpha_2)} * M_{Z3}$$

(Equation 6.19)

The maximum lateral force at the outer front tire is 3878.9 N (395.4 kg). The values used are obtained from the curve corresponding to 350 kg as this is closest to the value of 395.4 kg. It is shown in appendix E and are presented in table 6.7.

.

Table 6.7: Slip angle, lateral force and self-aligning torque values used in the interpolation

Slip angle [degrees]			Lateral force [N]			Self-aligning torque [Nm]	
$\boldsymbol{\alpha_1}$	-3.0		$\mathbf{F_{Y1}}$	3250.0		$\mathbf{M_{Z1}}$	-73.75
$\boldsymbol{\alpha_2}$	-4.0		$\mathbf{F_{Y2}}$	3687.5		$\mathbf{M_{Z2}}$	-70
$\boldsymbol{\alpha_3}$	-5.0		$\mathbf{F_{Y3}}$	4125.0		$\mathbf{M_{Z3}}$	-66.25

The slip angle at lateral force 3878.9 N:

$\alpha(3878.9\ N) = -4.437\ degrees \approx -4.4\ degrees$

The self-aligning torque at -4.8 degrees:

$M_Z(-4.4\ degrees) = -66.56\ Nm \approx -68.5\ Nm$

The pneumatic trail is then

$t_p = \frac{|M_Z|}{F_Y} = \frac{68.5\ Nm}{3878.9\ N} = 0.0177\ m = 17.7\ mm$

The resultant lateral force will be acting 17.7 mm behind the center of the tire as seen in figure ABCD below.

As the mechanical trail almost equals the pneumatic trail, the steering torque is dominated by both. This is desirable as a balance by both will give the driver a warning that the front wheels are nearing the limit. In a case with too little mechanical trail the pneumatic trail would dominate and reduce the self-centering steering torque. In an opposite case with too little pneumatic trail, the driver would not sense the input from the front steering wheels.

The offset arm (figure 6-9) is designed to point 39.3 degrees inwards. The inclined length is 110 mm where the distance to the center of the hole is 103.4 mm. The corresponding horizontal lengths are respectively 85.2 mm and 80 mm. With the hole in this position, the steering rack is placed 50 mm from the front frame to assure 90 degrees angle for the tie rod.

For comparison considerations, horizontal lengths of 60 mm and 70 mm of the offset arm have been used when calculating the tie rod forces.

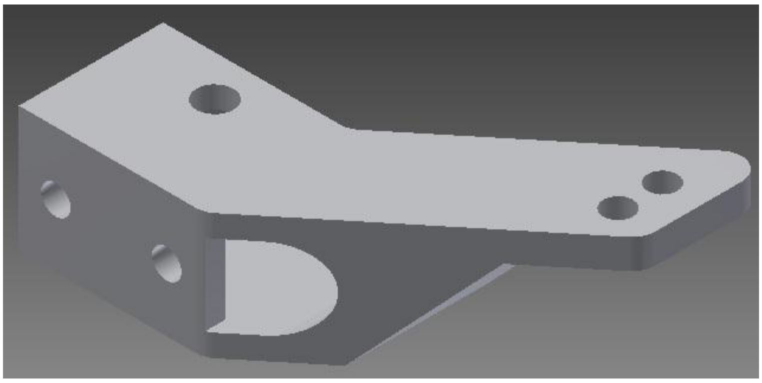

Figure 5-9: Offset arm

The force acting on the tie rod can be found by using force equilibrium as seen in figure XX:

$$F_y * a = F_s * b \qquad \text{(Equation 6.20)}$$

where
F_y: Lateral Force = 3878.9 N (from table 6.5)
F_s: Force acting on tie rod
a: Mechanical trail + pneumatic trail distance = 21.9 mm + 17.7 mm = 39.6 mm
b: Horizontal distance on the offset arm from where the lower a-arms connects and to the tie rod. (60mm, 70mm, 80 mm)

$$F_s = \frac{F_y * a}{b} \qquad \text{(Equation 6.21)}$$

$$F_s = \frac{3878.9\ N * 39.6\ mm}{b\ [mm]} = \frac{153604.4\ kNmm}{b[mm]}$$

From equation 6.21 it can be seen that the force on the tie rod will decrease as b increases; hence the force will decrease as the rod end is connected further to the outmost end of the connection point.

The steering rack was also placed as close as possible to the front frame to decrease the angle between the tie rod and the steering rack. As the angle decreases, the momentum that will build up will decrease. The best position for the steering rack will be where the angle of the tie rod is 90 degrees, relative to the horizontal axis (figure 6-10).

Three distances from the front frame was analyzed to find the best placement.

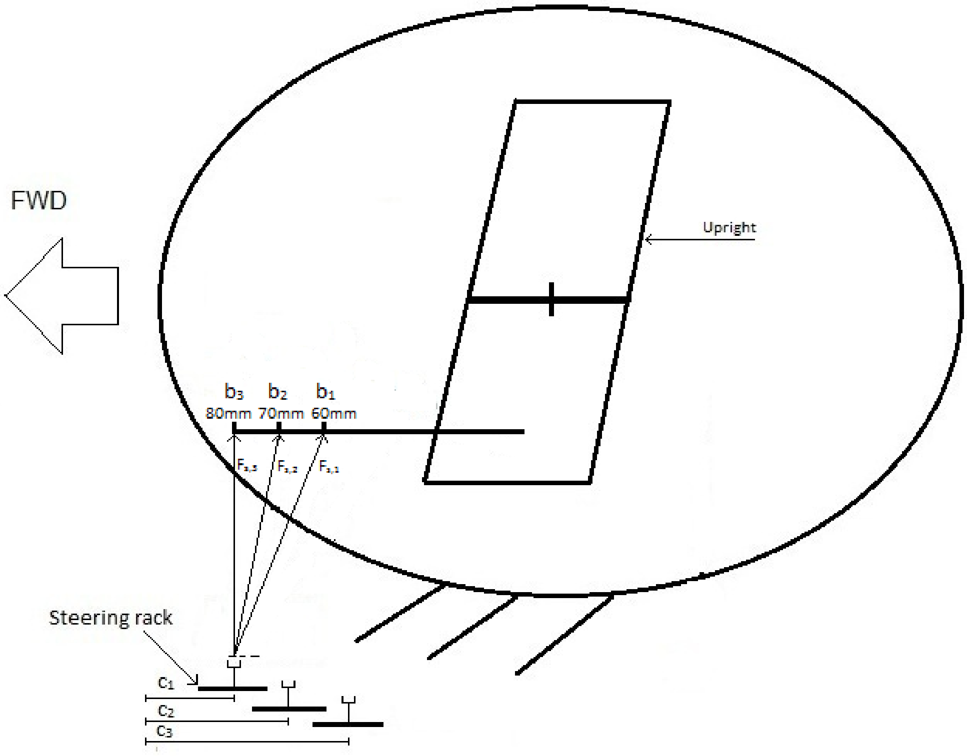

Figure 5-10: Different positions for the steering rack

Table 6.8: Tie rod forces at distance b from the wheel center, and distance c from front frame

Steering rack at a distance 60 mm (C_3) from the front frame			
			F_s [N]
Distance b	**b_1 [mm]**	60	2561.55
	b_2 [mm]	70	2194.35
	b_3 [mm]	80	1921.30
Steering rack at a distance 50 mm (C_2) from the front frame			
			F_s [N]
Distance b	**b_1 [mm]**	60	2565.98
	b_2 [mm]	70	2195.69
	b_3 [mm]	80	1920.06
Steering rack at a distance 40 mm (C_1) from the front frame			
			F_s [N]
Distance b	**b_1 [mm]**	60	2573.38
	b_2 [mm]	70	2199.71
	b_3 [mm]	80	1921.30

The tie rod will have the smallest force (1920.1 N) at a distance of 50 mm from the frame at an angle of 90 degrees.
The rod end will connect at a distance of 80.0 mm (100 mm) on offset arm.

5.4.3 Bolt Calculation

The bolt is affected by both shear forces and a momentum force. As the momentum will have the biggest impact on the bolt, the calculations have been done to see if the bolt can withstand the momentum force.

A chin of 15 mm takes up the moment and the bolt area through the chin is unthreaded. The bolt diameter is 8 mm with 12-9 quality.

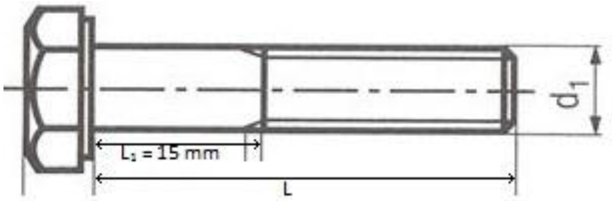

Figure 5-11: Bolt M8, 12-9 quality

NS-EN-1993-1-1:2005+NA:2008 fomulas:

$$\frac{M_{Ed}}{M_{c,Rd}} \leq 1{,}0 \qquad \text{(Equation 6.22)}$$

$$M_{c,Rd} = M_{el,Rd} = \frac{W_{el,min} * f_y}{\gamma_{M0}} \qquad \text{(Equation 6.23)}$$

where f_y = 1080 MPa, γ_{M0}= 1.05

$$W_{el,min} = \frac{I}{z_{max}} \qquad \text{(Equation 6.24)}$$

$$I = \frac{\pi * D^4}{64} = \frac{\pi * 8.0^4}{64} = 201.0619\ mm^4$$

$$z_{max} = \frac{8.0mm}{2} = 4.0\ mm$$

$$W_{el,min} = \frac{201.0619\ mm^4}{4.0\ mm} = 50.265\ mm^3$$

$$M_{c,Rd} = \frac{50.265\ mm^3 * 1080\frac{N}{mm^2}}{1.05} = 51701.1\ Nmm$$

For M_{ED} a security factor of 1.5 is used. The chin length is 15 mm:

$$M_{Ed} = F_s * L_1 = 1920.1\ N * 1.5 * 15\ mm = 43202.3\ Nmm$$

Checking due to equation 6.22:

$$\frac{M_{Ed}}{M_{c,Rd}} = \frac{43202.3}{51701.1} = 0.836$$

An M8 bolt will resist the momentum.

With the same calculations for a M6 bolt of 12-9 quality the results shows that the bolt will not resist the momentum. An M8 bolt will therefore be used.

5.4.4 Rod End

The rod end consists of a spherical bearing that will prevent a torque from occurring. As an M8 bolt had to be used to withstand the momentum when connecting the rod end to the offset arm (section 6.4.3), a rod end of minimum 8 diameters has to be used. SKF offers different rod ends (Appendix H) which can withstand different static and dynamical load ratings.

A M8 rod end was used resisting maximum load of 5850 N and maximum static load is 12 900 N. The force acting on the tie rod with a safety factor of 1.5 is F_s = 2880.2 N.

This is a suitable rod end, and 4 rod ends will be used; 1 on each end of the tie rods.

5.4.5 Tie rod

The tie rod was designed to resist buckling and is made of 4130 steel. The steel was bought from Aerocom Metals, and a certificate, test result and products list are attached as appendices (appendix I). The dimensions are shown in figure 6-12 below:

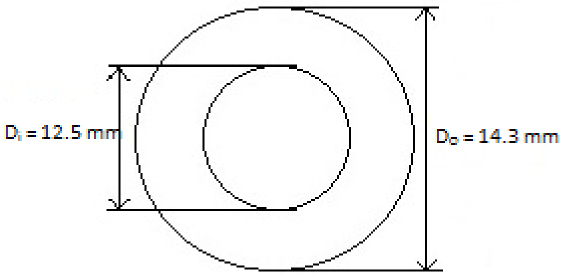

Figure 5-12: Dimensions of the tie rod

NS-EN-1993-1-1:2005+NA:2008 fomulas:

The criteria to resist buckling is

$$\frac{N_{Ed}}{N_{b,Rd}} \leq 1{,}0 \qquad \text{(Equation 6.25)}$$

N_{Ed} is 2880.2 N which is the force acting on the tie rod with a safety factor of 1.5.

Radii of gyration:

$$i = \sqrt{\frac{I}{A}} \qquad \text{(Equation 6.26)}$$

Moment of Inertia:

$$I = \frac{\pi}{64}[\,(D_o)^4 - (D_i)^4\,] \qquad \text{(Equation 6.27)}$$

$$I = \frac{\pi}{64}[\,(14.3\,mm)^4 - (12.5\,mm)^4\,] = 854.223\,mm^4$$

Cross-section area:

$$A = \frac{\pi}{4}\,(D_o)^2 - \frac{\pi}{4}\,(D_i)^2 \qquad \text{(Equation 6.28)}$$

$$A = \frac{\pi}{4}\,(14.3\,mm)^2 - \frac{\pi}{4}\,(12.5\,mm)^2 = 37.888\,mm^2$$

From equation 6.26:

Radii of gyration:

$$i = \sqrt{\frac{854.223\ mm^4}{37.888\ mm^2}} = 4.748\ mm$$

Non-dimensional slenderness:

$$\overline{\lambda} = \frac{L_{cr}}{i} * \frac{1}{93.9*\varepsilon} \qquad \text{(Equation 6.29)}$$

$$\varepsilon = \sqrt{\frac{235}{f_y}}$$

where L_{cr} = L = 350 mm (appendix J), f_y =650 MPa

$$\varepsilon = \sqrt{\frac{235}{650MPa}} = 0.601$$

From equation 6.29:

$$\overline{\lambda} = \frac{350\ mm}{4.748} * \frac{1}{93.9*0.601} = 1.306$$

Hollow section, hot rolled, graph a) (see appendix J)

$$\phi = 0{,}5 * [\ 1 + \alpha\left(\bar{\lambda} - 0{,}2\right) + \bar{\lambda}^2\ ]$$

$$\alpha = 0.49$$

$$\phi = 0.5 * [1 + 0.49\ (1.306 - 0.2) + 1.306^2] = 1.624$$

Reduction factor:

$$\varkappa = \frac{1}{\phi + \sqrt{\phi^2 - \overline{\lambda}^2}}$$

$$\varkappa = \frac{1}{1.624 + \sqrt{1.624^2 - 1.306^2}} = 0.386$$

Buckling resistance:

$$N_{b,Rd} = \frac{\varkappa * A * f_y}{\gamma_{M1}} \qquad \text{(Equation 6.30)}$$

$$N_{b,Rd} = \frac{0.386*37.888\ mm^2*650\ \frac{N}{mm^2}}{1.05} = 9053.4\ N$$

Checking the criteria:

$$\frac{N_{Ed}}{N_{b,Rd}} = \frac{2880.2\ N}{9053.4\ N} = 0.318$$

The tie rod will resist buckling with the given dimensions.

5.4.6 Quick Release Fastening and Position

A Sparco quick release/snap off is mounted through the dashboard and connected onto a hollow column acting as a bearing house which is welded to the frame. Two single row deep groove ball bearings (d_i=20 mm and d_o=42 mm), (appendix K) are placed inside the bearing house for stabilization to the quick release axle when turning the steering wheel.

One rule stated by the SAE says that "In any angular position, the top of the steering wheel must be no higher than the top-most surface of the Front Hoop". This rule gives restrictions to the height of the quick release and the steering wheel. The position should be as high as possible to give more space for the driver. Figure 6-13 shows the dashboard dimensions and the highest position possible for steering wheel that complies with the rules. The position has been obtained by making an assembly of the steering wheel mode, dashboard model and the frame model.

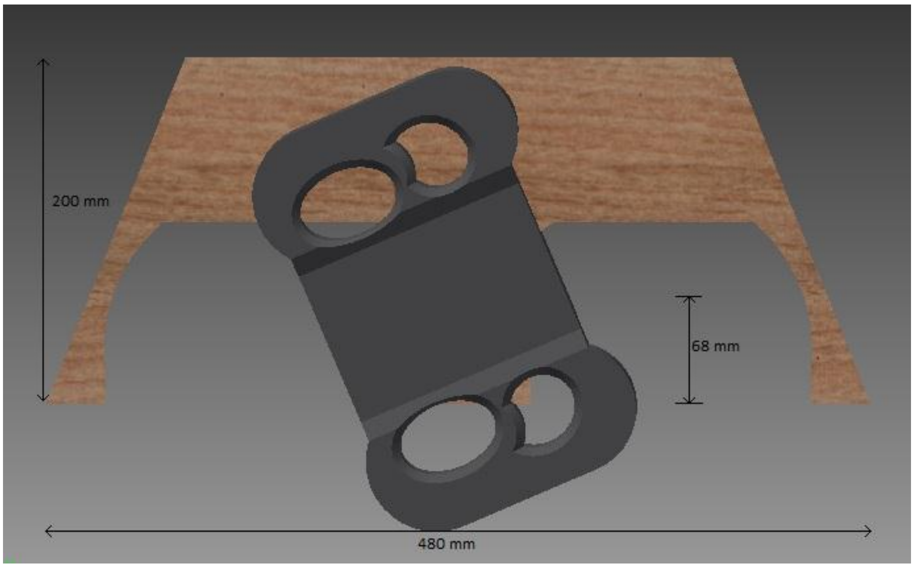

Figure 5-13: The position of the steering wheel on the dashboard

5.4.7 The Design's Influence On The Car

It is of interest to see how the design affect the car's handling and performance.

With the body and wing added to the car, a bigger amount of space is required in a turn (figure 6-14). In the skid-pad event the circles has a radius of 7625 mm and the distance between the cones is 3 meters. The required space needed for the car can be expressed by ΔR by equation

$$\Delta R = R_{max} - R_{min} \qquad \text{(Equation 6.31)}$$

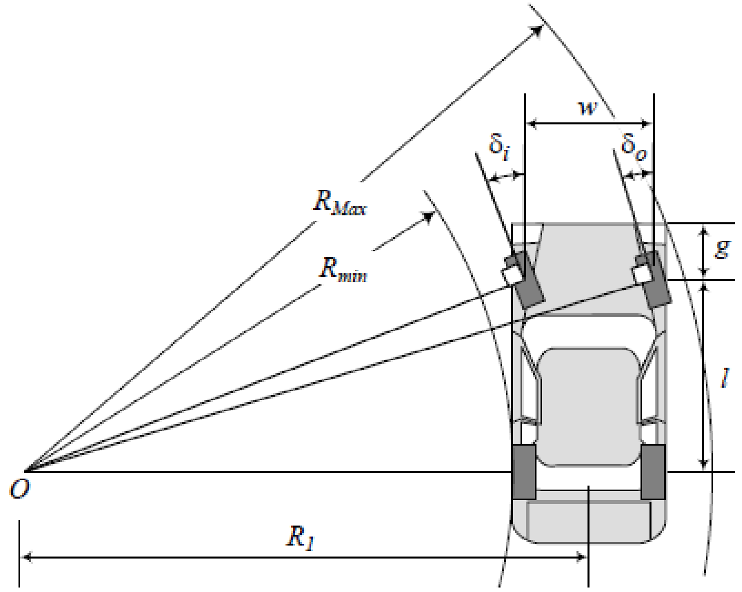

Figure 5-14: Space required in a turn

R_{min} represents the distance from the turn center to the inner rear wheel and is expressed by

$$R_{min} = R_1 - \frac{w}{2} \qquad \text{(Equation 6.32)}$$

R_1 was calculated to 7582.9 mm (section 6.4.1) and hence

$$R_{min} = 7582.9\ mm - \frac{1290\ mm}{2} = 6937.9\ mm$$

R_{max} represents the distance from the turn center to the outer point of the front wing/body and is the biggest running radius required. With the outer point at a distance g from the front axle, it can be expressed by

$$R_{max} = \sqrt{(R_{min} + w)^2 + (l + g)^2} \qquad \text{(Equation 6.33)}$$

$$R_{max} = \sqrt{(6937.9\ mm + 1290\ mm)^2 + (1600\ mm + 1250\ mm)^2} = 8707.5\ mm$$

The required space in the turn is

$$\Delta R = 8707.5\ mm - 6937.9\ mm = 1769.6\ mm$$

6 ANALYSIS AND SIMULATIONS

The design has been simulated and analyzed in MSC ADAMS, a multi-body simulation program, to compare the theoretical values with the values from the multi-body simulation. It also shows how the steering system acts during operation of the car.

ADAMS (Automated Dynamic Analysis of Mechanical Systems) is a multi-body dynamics software used to study and simulate the dynamics of moving parts. By offering different packages for different areas of simulation, better simulations and more accurate results are obtained.

The 2013 formula student team is sponsored with an ADAMS/car package to be used in the two Master Thesis. The program has been learned simultaneously with the process of building the car, as the University of Stavanger offers no education in the program.

For the study of the formula 2013 car, ADAMS/Car package is used to study the car's behavior in handling, steering and during braking.

6.1 Multi-body simulation model

A multi-body simulation model is an assembly of different subsystems converted from templates. A template defines how the parts fit together (the topology) and how the information is transmitted between them in the model. The template has a defined major role (suspension, steering etc.).

The template is converted to a subsystem which is a mechanical model that supplies parameters to the template. Front- and rear suspension and steering subsystems are some examples. To be able to use the same template for different subsystems, the minor role of the subsystem is defined as front, rear, trailer or any when it is created.

Assemblies are used to connect different subsystems together with a test rig. The test rig is important as it imposes motion to the subsystem to be able to do simulations and analysis.

MSC Adams is offering a special FSAE database compatible with Adams/car. The database contains templates and subsystems of a formula student car which can be modified by the formula student teams to represent their own car and used for analyses of each individual car.

To represent the 2013 formula student car and analyze the steering system, the fsae_2012 front suspension template has been modified. The modification has been done by changing parameters of radius, material etc. and by changing the coordinates of the hardpoints. The coordinates have been obtained by using information from another master thesis on the same formula student 2013 racing car, as this thesis are dealing with the design of the suspension system. To be able to modify the template, the .acar.cfg-file has been changed from standard user mode to expert user mode.

The hardpoints are given to the program as coordinates and gives the program information about the location. However, as they are only points they have no orientation. Link or arm geometry is added from one hardpoint to another to obtain the preferred geometry in the multi-body model. Only the left hardpoints were modified as seen in table 7.1, as they were defined symmetrically which automatically updates the right hardpoints relative to the x,y,z axis.

Table 7.1: Left side hardpoints for the multi-body model

Type	Hardpoint name		Coordinates
Lover control arms/A-arms	From:	L_arm_outer	(-512.0, 571.7, 27.4)
	To 1:	L_arm_front	(-630.3, 229.0, 22.4)
	To 2:	L_arm_rear	(-393.7, 229.0, 22.4)
Upper control arms/A-arms	From:	U_arm_outer	(-492.8, 710.9, 247.4)
	To 1:	U_arm_front	(-630.3, 279.0, 183.4)
	To 2:	U_arm_rear	(-355.3, 279.0, 183.4)
Tierod	From:	tierod_outer	(-572.8, 510.9, 47.4)
	To:	tierod_inner	(-572.8, 350.0, 47.4)
Pushrod	From:	prod_outboard	(-512.0, 571.8, 27.4)
	To	prod_inboard	(-512.0, 309.2, 482.1)
Rocker/Damper	From:	BC_center	(-512.0, 213.9, 427.1)
	To:	damper_outboard	(-512.0, 240.0, 550.0)
	To:	damper_inboard	(-131.0, 90.0, 600.0)

6.1.1 Upper control arms

The upper control arms are made by link geometry, from U_arm_outer to U_arm_front, and from U_arm_outer to U_arm_rear. As the diameter is 15.875 mm, the radius is set to 7.9375 mm. The material type is set to steel.

6.1.2 Lower control arms

The lower control arms are also made by link geometry, starting at L_arm_outer to L_arm_front, and from L_arm_outer to L_arm_rear. The diameter is 22.225 mm, the radius is set to 11.1125 mm. The material type is set to steel.

6.1.3 Tie rod

A link connection from tierod_outer to tierod_inner with a radius of 7.15 mm is defining the tierod. The tierod is connected from the steering rack to the upright on the wheel and are moving when the steering wheel is turning and this turns the wheel.

6.1.4 Pushrod

The pushrod is made by a link connection from prod_outboard to prod_inboard with a radius of 9.525 mm. The pushrod is connected to the L_arm_outer, the outer point of the lower a-arms. As the wheel travel upwards the pushrod are pushing on the rocker which compresses the damper.

6.1.5 Rocker/Damper

The rocker is defined as an arm geometry and is fixed to the frame at hardpoint BC_center. It rotates relative to this hardpoint as the pushrod pushes it.

6.1.6 Communicators

Communicators enable the exchange of information between templates, subsystems and the test rig in the assembly. Input and output communicators are requesting and providing information from other subsystems.

A mount communicator in the steering template outputs the name of the rack so the tierod on the suspension template can attach to it. In the steering template, a mount communicator inputs a part name as the template uses this name to determine the attachment of the steering column.

6.1.7 Actuators

To let an element apply motion to components in the model, actuators are defined. An actuator is used for the pushrod and the rocker, and the rocker and the damper to let them exert motion on each other. This is also the case between the tierod and steering link.
The motion actuator is called a joint.

The template is saved and converted to a subsystem (appendix L, figure L.1). The minor role for the new subsystem is set to “front” as it is designed as a front suspension system. It is also important to choose “front” as this tells ADAMS to connect it to the fsae_2012 steering subsystem later.

6.2 Driving/Steering simulation

An assembly (appendix L, figure L.2) was created including the front suspension subsystem (section 7.1) and fsae_2012 steering subsystem. A standard test-rig was used.

As the steering subsystem was made for a standard Formula Student car, the position of the steering rack would be off to the position of the tie rods. When visualizing the assembly it would look wrong as the steering rack would be placed far behind the tie rods. However, as mount communicators are used they would still connect to each other and work correctly.

For visualization purposes, the hardpoints on the steering subsystem was moved to positioning it correctly to the tie rods.

6.2.1 Steering angles and forces

A analyze was made of the steering system where the steering rack moved 10 mm towards the right. The car was at rest only turning the wheels. From the reversed Ackermann theory, a right turn should lead to the outer wheel turning at a bigger angle compared to the angle of the inner wheel. This is confirmed by the analysis (appendix M, figure M.1). The left and right wheels got an angle of respectively 10.53 degrees and 8.46 degrees.

The force on the steering rack increases from 0 N to 156.91 N as the wheels are moving to the right (appendix M, figure M.2).

By shortening the offset arm, the steering angles and forces are changing. In section 6.4.2 the equation

$$F_s = \frac{F_y * a}{b}$$

were used to calculate the force exerted on the tie rod and the steering rack where "b" were expressing the horizontal distance on the offset arm from where the lower a-arms connects and to the tie rod. By shortening the offset arm "b" the force needed to turn the wheels should increase. The steering angle is also increasing as the tie rod is connected closer to the center of the wheel. The results can be seen in appendix M, figure M.3, M.4 and M.5.

6.3 Sensitivity Analysis

6.3.1 Cornering

A cornering maneuver was simulated and analyzed. The cornering forces were calculated in section 6.3.3 and it was applied 3878.9 N to the left wheel and 1500.5 N to the right wheel. As the steering rack was moving 20 mm to the right, a force of 1390.94 N was exerted on the tie rods (appendix M, figure M.6). This is well below the design force of 2880.2 N which were used for the design.

6.3.2 Braking

For the braking simulation, a value of 3895.5 N from section 6.3.4 was used on the front wheels. As the steering rack was moving 20 mm to the right, a force of 3638.07 N was exerted on the tie rods (appendix M, figure M.7). This is higher than the design force and a new buckling analysis was done. By checking for the buckling criteria;

$$\frac{N_{Ed}}{N_{b,Rd}} = \frac{3895.5\ N}{9053.4\ N} = 0.43$$

The tie rod fulfills the criteria and will resist buckling.

6.4 Failure Mode and Effect Analysis (FMEA)

The designation “steering system” refers to the steering system as a whole. The system can be divided into sub-systems where each sub-system has its own role. As an example, the offset arms are a sub-system in which their role is to connect the tie rods to the upright on the wheel. Bolts and nuts are another sub-system with the function of holding parts in a specific position.

Each component in the sub-system is subjected to wearing and tearing as the system is operating. The operational environment and conditions affects the amount and type of the wearing.

In the process of determining the risk of a failure and the cause, a Failure Mode and Effect Analysis (FMEA) is used. The analysis is a systematic and proactive way to identify the failure modes, the effect and how it can be prevented.

Each sub-system is analyzed and evaluated to find the effect a failure would have on the rest of the system. The likelihood of occurrence is scaled from 1 – 10 (10: very likely to occur), the likelihood of detection is scaled from 1 – 10 (10: very unlikely to detect) and the severity is scaled from 1 – 10 (10: most severe effect). Each failure mode is given a Risk Priority Number (likelihood of occurrence x likelihood of detection x severity) where a high number has a big effect on the process and should have a high priority when it comes to control. A low RP-number indicates a low effect on the process and has lower priority.

The steering system was analyzed part-by-part to find causes of failures and effects. The analysis can be seen in Appendix FMEA.

The offset arms are not stated in the analysis as they were considered to be in the safe area of operation. They were designed to withstand a bigger amount of load than will occur during the race.

The analysis gives a total RPN of 344 points. The movement of the quick release axle consists of almost ¼ of the total RPN with the highest score of 81 points. The disconnection of the steering wheel has a score of 60 points and the failure of the rack and pinion gear has 50 points. These are the three most important areas to control to assure a safe and reliable steering system and should be given high priority.

6.5 Cost and Weight Analysis

One of the main goals for the team is to decrease the weight wherever possible and hence decrease the total weight which will provide a lighter, faster and more maneuverable car for the competition. This is obtained by considering the materials available and the manufacturing process used. The area in which the material is connected is also of importance, as aluminium cannot be welded directly to the steel frame.

The budget for the steering system was set to 5500 NOK and shown in appendix O. It was considered to use the same quick release mechanism as last year's team but it was later decided to be impossible to do this. A new mechanism was ordered which made it one of the biggest expenses.

It was also considered to order a light-weight steering rack in carbon fiber (figure 7-1) from Formula Seven, a Formula Student team manufacturing and selling light-weight products. The specifications are shown in table 7.2 below.

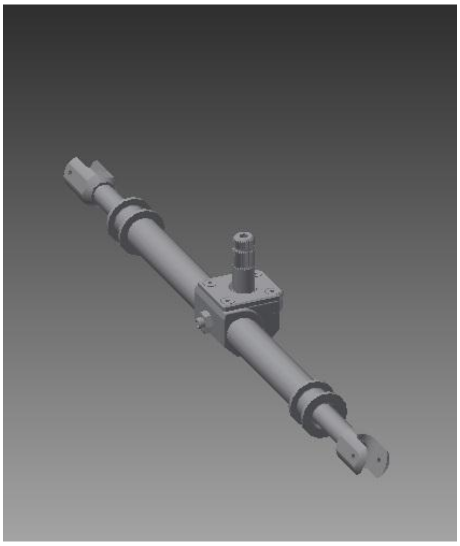

Figure 6-1: Carbon fiber steering rack from Formula Seven

Table 7.2.: Steering racks specifications

Overview of the compared steering racks			
Manufacturer	**Material**	**Weight**	**Price**
Formula Seven	Carbon Fiber / Aluminium	950 grams	800 EUR = 5984 NOK (1 EUR = 7.48 NOK (23.02.2013))
IC-Kart	Aluminium	1180 grams	1500 NOK

Due to restrictions in the budget, a steering rack from IC-Kart was ordered (figure 7.2).

Figure 6-2: Aluminium steering rack from IC-Kart

For welding purposes, thin steel plates were used when fastening the steering rack as it was welded to a steel frame. This was also the case when fastening the quick release mechanism. Steel was also used for the tie rods. The offset arms were manufactured in aluminium at the school's workshop location and were designed for minimum weight.

The total cost of the steering system was 6228 NOK, 728 NOK more than the budget (appendix O). The order of a new quick release mechanism made a huge influence of the budget making it impossible to stay on the budget. The same steering wheel and shifter pads were used to save money.

6.6 Testing methods for the steering system

Understeer and oversteer are defined by a understeer gradient K and can be tested on a testing track. How the steering needed for a steady turn changes is measured by a gradient K as a function of lateral acceleration. If K is positive the vehicle shows understeer, if it is negative the vehicle shows oversteer. Constant radius tests at different speeds, constant speeds at different steer angles or constant steer at different speeds can be done.

A Bundorf analysis can also be carried out to describe the characteristics of a vehicle and its understeer balance. The car is analysed and a summation of aligning torque, roll camber, roll steer and lateral force in deg/g at front and rear axle is done. If the sum is negative the vehicle will tend to oversteer.

7 CONCLUSIONS AND RECOMMENDATIONS

7.1 Conclusions

The Formula Student project has been challenging and time consuming as the car is manufactured and build at the same time the Master Thesis is written. It has also been giving valuable practice in team work and project design.

The car has not been tested as major issues with the clutch system appeared before shipping it to the Silverstone circuit. The steering system will therefore be tested at the circuit.

7.2 Recommendations

Better tire test-results should be available to gain better estimates for the racing car. The 2014 team should pay to get access to the tire consortium. This will also give a better feedback if we are using the correct tires or should change to another type.

It should also be budgeted for a set of new 10 inch wheels as this would lower the weight of the car. It is also preferable to buy a lighter steering rack. If the team is bigger next year, a light-weight steering rack could also be made.

Students should learn a multi-body dynamics software before writing thesis for the Formula Student competition. This will make it easier to make good decisions and lock the design in an early phase, so the car can be finished earlier.

REFERENCES

- 2012/2013 formula SAE Rules
- SAE J670, Vehicle Dynamics Terminology
- http://www.millikenresearch.com/fsaettc.html (26.02-2013)
- A. van Berkum, Chassis and suspension design FSRTE02, March 2006, Master Thesis
- Hagerman. John, Grassroots Motorsports Magazine
- http://dukemotorsports.blogspot.no/2011/07/aerodynamics-and-vehicle-dynamics.html

BIBLIOGRAPHY

- William F. Milliken and Douglas L. Milliken (2003), Race Car Vehicle Dynamics, pld. SAE International
- Associate Professor. Siriwardane. S. Chaminda, *Steel Structures lecture notes*, 2012
- Smith. D. Nicholas (2004), Understanding Parameters Influencing Tire Modeling, Colorado State University
- Swiss Federal Institute of Technology Zurich, Vehicle dynamics and design lecture notes http://www.idsc.ethz.ch/Courses/vehicle_dynamics_and_design/11_0_0_Steering_Theroy.pdf
- Institute for Healthcare Improvement, 2004 lecture notes http://medqi.bsd.uchicago.edu/documents/FailureModesandEffectsAnalysis_FMEA_1.pdf
- Jazar, Reza N. (2008), Vehicle dynamics: theory and applications. Springer. P. 11.
- http://www.hoosiertire.com/ 21.02.2013

INTERNET SITES

- http://www.formulastudent.com/aboutus/thechallenge 30.01.2013
- http://www.tpub.com/ 05.02.2013
- http://www.britannica.com/EBchecked/topic/473389/power-steering 05.02.2013
- http://www.auto-ware.com/setup/toe_hand.htm 12.01.2013
- http://www.smithees-racetech.com.au/ackerman.html 12.01.2013
- http://www.ehow.com/about_6502053_manual-steering-vs_-power-steering.html 23.02.2013
- http://skfwebtools.com/GC6000/iec?maincatalogue=1&lang=en&newlink=3_3_21 26.02.2013
- http://www.millikenresearch.com/fsaettc.html 26.02.2013
- http://www.dani-tech.com/produkter/forbrugsvarer/boltevare/bolte/din-931/0057-bolt-6-kant_.aspx?lang=uk 14.03.2013

Appendix A

Master Thesis specification

Project description of Master thesis
<u>Christoffer L. Andersen</u>

1. Title of Thesis:
   Modeling, analysis and testing of The Steering system in a Formula Student car FS_UiS2013

2. Background for the task:

   The task is based on the Formula Student (FS) project at UiS that started 2 years ago and I am member of this year's team.

3. Goal of the task:

   The goal of the thesis work, as part of the FS project, is to contribute in an effective steering and focuses on ***design, analysis and simulation of the system***.

4. Scope (description of content, theoretical backgrounds, literature, etc..):

Being part of the overall construction of the race car, the tasks of this master thesis project work involve, among others

1. Studying the important components and design parameters of the race car steering system with particular focus on how to achieve safe and reliable steering system.
2. Developing a multi-body simulation (MBS) model for virtual simulation of the steering system. This involves learning a MBS tool such as MSC ADAMS and using it to simulate steering linkage.
3. Devising a simulation scheme that closely simulates the real driving/steering situation and identifying the key performance parameters for this purpose.
4. Making a sensitivity analysis of the designed steering system with respect to how the steering mechanism responds to the actions of the driver, for instance, in cases of accelerating, braking, cornering, etc.
5. Studying the test setup for testing of over/under steering of the car. The test setup must be done in a way to be able to verify some of the simulation results.
6. Studying the relevant competition rules concerning the steering system and preparing the necessary documentations that are part of the requirements for the completion. Such documentations must be included in the thesis report as appendices.
7. Studying the principle of FMEA (Failure Mode and Effect Analysis) and working out the form for the steering system. The FMEA form must be included in the thesis report as an appendix.

Appendix B

Pre-study Report

Pre-project for the master thesis «Modeling, analysis and testing of the steering system in a formula student car FS_UiS 2013»

The Master Thesis will take part in spring 2013 and focus on the steering system on a formula student racing car. It will be as much practical as theoretical as the steering system has to be installed in the car, and other aspects as suspension, uprights and wheels have to be considered as well.

The planning face started in October with meetings, design brainstorming and sponsors inquiries. The project needed funds to be able to build the desired racing car. This has been the focus since October.

The project is divided into different groups, each with its own area of focus. The project has been assigned its own room where the groups are sitting to give better teamwork and communication. An own electrical engineering-group has been assigned and they are sitting on another building. Therefore, all the groups are meeting every Tuesday from 12:15 – 13:00 to discuss and inform about their progress.

For the Master Thesis, the following problem formulations were given:

1. Studying the important components and design parameters of the race car steering system with particular focus on how to achieve safe and reliable steering system
2. Developing a multi-body simulation (MBS) model for virtual simulation of the steering system. This involves learning a MBS tool such as MSC ADAMS and using it to simulate steering linkage.
3. Devising a simulation scheme that closely simulates the real driving/steering situation and identify the key performance parameters for this purpose.
4. Making a sensitivity analysis of the designed steering system with respect to how the steering mechanism respond to the actions of the driver for instance in cases of accelerating, braking, cornering, etc
5. Devising a test setup for testing of over/under steering of the car. The test setup must be done in a way to be able to verify some of the simulation results.
6. Studying the relevant competition rules concerning the steering system and preparing the necessary documentations that are part of the requirements for the completion. Such documentations must be included in the thesis report as appendices.
7. Studying the principal of FMEA (Failure Mode and Effect Analysis) and working out the form for the steering system. The FMEA form must be included in the thesis repost as an appendix.

The Gantt chart illustrates the time schedule for the Master Thesis progress. A literature search has been done and the focus is on different concepts and calculations to find the best solution.

In March, MSC ADAMS will be used to do analysis and simulations of the steering linkage, driving/steering and sensitivity. The report will be made simultaneously. The frame is welded in January/February and the body will be made in March. Therefore, I assume that the installation process of the steering system will take place in April. Changes on time schedule may occur.

The resources used are literature explaining the concept of steering systems and suspension. I will also study tire behavior.

Some parts of the steering system may be manufactured. This can be done at the University, or we may contact a sponsor who has accepted to help with manufacturing, to do the most advanced parts.

31.01-2013, Stavanger

Christoffer L. Andersen

Modeling, analysis and testing of the steering system in a formula student car FS_UiS 2013

TIME SCHEDULE

ID		Task Name	Duration	Start	Finish
1		**Master Thesis**	**159 days**	**Mon 07.01.13**	**Fri 14.06.13**
2		Semester start at UiS	0 days	Mon 07.01.13	Mon 07.01.13
3		Talk to the supervisor	1 hr	Mon 07.01.13	Mon 07.01.13
4		Meet the project group	7 days	Mon 07.01.13	Sun 13.01.13
5					
6		**Preproject**	**15 days**	**Mon 14.01.13**	**Mon 28.01.13**
7		Master Thesis problem formulation	5 days	Mon 14.01.13	Fri 18.01.13
8		Literature search	4 days	Fri 18.01.13	Mon 21.01.13
9		Information meeting with supervisor	2 hrs	Tue 22.01.13	Tue 22.01.13
10		Handing in preproject report	0 days	Thu 31.01.13	Thu 31.01.13
11		Signing the Master Thesis problem formulation	0 days	Thu 31.01.13	Thu 31.01.13
12					
13		Official start on Master Thesis	0 days	Fri 01.02.13	Fri 01.02.13
14					
15		**Concept development**	**37 days**	**Wed 23.01.13**	**Thu 28.02.13**
16		Literature study	18 days	Sun 20.01.13	Wed 06.02.13
17		Concepts and calculations	24 days	Wed 06.02.13	Fri 01.03.13
18					
19		**Analysis and Simulations**	**31 days**	**Fri 01.03.13**	**Sun 31.03.13**
20		Steering linkage simulation	10 days	Fri 01.03.13	Sun 10.03.13
21		Driving/Steering simulation	10 days	Mon 11.03.13	Wed 20.03.13
22		Sensitivity analysis	7 days	Thu 21.03.13	Wed 27.03.13
23					
24		**Building and adjustment**	**61 days**	**Mon 01.04.13**	**Fri 31.05.13**
25		Manufacture and installation	31 days	Mon 01.04.13	Wed 01.05.13
26		Adjustments	31 days	Wed 01.05.13	Fri 31.05.13
27					
28		**Report**	**152 days**	**Mon 14.01.13**	**Fri 14.06.13**
29		Writing draft version	108 days	Mon 14.01.13	Wed 01.05.13
30		Talk to the supervisor	2 hrs	Wed 01.05.13	Wed 01.05.13
31		Modify draft version	45 days	Fri 03.05.13	Sun 16.06.13
32					
33		**Handing in Master Thesis**	**0 days**	**Fri 14.06.13**	**Fri 14.06.13**

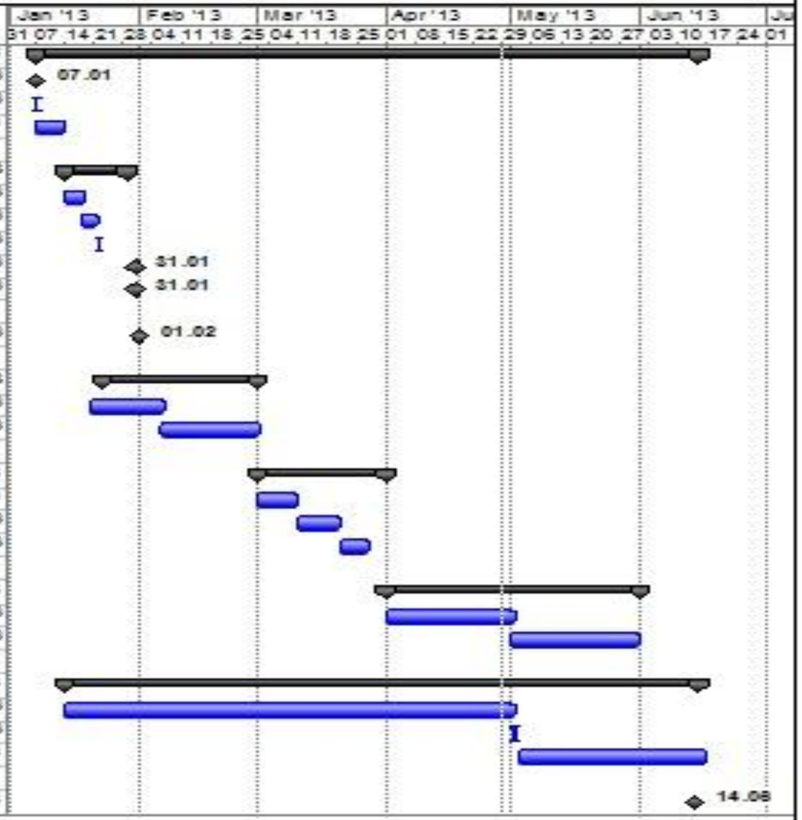

Project: Master Thesis Preproject repo

Task		Milestone		External Tasks	
Split		Summary		External Milestone	
Progress		Project Summary		Deadline	

Appendix C

Formula Student SAE Rules

FORMULA SAE SAE International

2013 Formula SAE® Rules
Table of Contents

2013 Formula SAE Rules
INTRODUCTION

This introduction highlights some areas of the 2013 Formula SAE rules that teams should understand and consider. This introduction only summarizes parts of the rules the revised text and do not change or replace the rules.

Caution – Neither this introduction, nor any other summary, is a substitute for reading and understanding the Rules. The Rules are both a controlling and a reference document and should be used for those purposes. Do not attempt to design your car based on the parts of the Rules you happen to remember from the last time you read them. We cannot stress it too strongly – Read the Rules thoroughly and repeatedly.

Revised Part Designations - The designations of some of the Parts of the FSAE Rules have been revised to better indicate their contents. The new designations are:

Part A – Administrative Regulations
Part T – General Technical Requirements
Part AF – Alternate Frame Rules
Part IC – Internal Combustion Engine Vehicles
Part EV – Technical Regulations - Electric Vehicles
Part S – Static Event Regulations
Part D – Dynamic Event Regulations

Part EV - Electric Vehicles - The most significant change to the 2013 Formula SAE Rules is the addition of regulations and requirements for electric vehicles. Section EV is largely based on the rules for the electric classes at Formula Student (UK) and Formula Student Germany with modifications implemented following a review by an international group of electric engineering experts. Many of the EV requirements will be familiar to teams that have participated in electric competitions.

A5.2 Electrical System Officer– Electric Teams Only – Electric teams are required to designate a person as their Electric Systems Officer who will be responsible for "all electric operations of the vehicle during the event."

A5.3 – Electric System Advisor – Electric Teams Only – Electric teams are required to designate an Electric System Advisor "who can advise on the safety systems to do with HV electrical configuration and control systems."

EV1.1.2 – Maximum Voltage – During the 2013 and 2014 Formula SAE competition years the maximum permitted nominal operational voltage is designated per competition.

EV9.1 - Electrical System Form (ESF) and EV9.2 - Failure Modes and Effects Analysis (FMEA) - Teams entering an electric vehicle are required to submit a detailed Electric Systems Form and an FMEA of the tractive system. Templates for these documents will be available online and must be followed.

T1.2 Steering – The steering regulations have been modified to clarify that the use of cable steering is permitted.

T3.10.4 on the location of the 95th percentile template - The location of the template in relation to the face of the pedals has been specified.

T5.6 Head Restraint – The head restraint regulations have been revised and clarified.

Part IC - Internal Combustion Vehicles – To simplify the rules we have separated the rules governing internal combustion vehicles from the general technical requirements.

S3.1 Business Logic Case – Each team is required to submit a brief "business logic case" which states the primary considerations and goals that influenced their design and fabrication choices. This submission replaces the Student Activity Disclosure Form.

C5.7 - **Student Activity Disclosure Form"** and all associated cross references including those in A8.1 "Required Documents and Required Forms" and A8.4 "Late Submission Penalties" – The requirement to submit the "Student Activity Disclosure Form" is eliminated.

D8.20 Fuel Efficiency – As listed in the 2012 "Notice of Possible Rule Changes" the Committee has voted to replace the Fuel Economy Event with a Fuel Efficiency Event. We suggest you thoroughly study the revised rules for this event.

T5.6.3 The restraint, its attachment and mounting must be strong enough to withstand a force of 890 Newtons (200 lbs. force) applied in a rearward direction.

T5.7 Roll Bar Padding

Any portion of the roll bar, roll bar bracing or frame which might be contacted by the driver's helmet must be covered with a minimum thickness of 12 mm (0.5 inch) of padding which meets SFI spec 45.1 or FIA 8857-2001.

T5.8 Driver's Leg Protection

T5.8.1 To keep the driver's legs away from moving or sharp components, all moving suspension and steering components, and other sharp edges inside the cockpit between the front roll hoop and a vertical plane 100 mm (4 inches) rearward of the pedals, must be shielded with a shield made of a solid material. Moving components include, but are not limited to springs, shock absorbers, rocker arms, anti-roll/sway bars, steering racks and steering column CV joints.

T5.8.2 Covers over suspension and steering components must be removable to allow inspection of the mounting points.

ARTICLE 6: GENERAL CHASSIS RULES

T6.1 Suspension

T6.1.1 The car must be equipped with a fully operational suspension system with shock absorbers, front and rear, with usable wheel travel of at least 50.8 mm (2 inches), 25.4 mm (1 inch) jounce and 25.4 mm (1 inch) rebound, with driver seated. The judges reserve the right to disqualify cars which do not represent a serious attempt at an operational suspension system or which demonstrate handling inappropriate for an autocross circuit.

T6.1.2 All suspension mounting points must be visible at Technical Inspection, either by direct view or by removing any covers.

T6.2 Ground Clearance

Ground clearance must be sufficient to prevent any portion of the car, other than the tires, from touching the ground during track events. Intentional or excessive ground contact of any portion of the car other than the tires will forfeit a run or an entire dynamic event.

Comment: The intention of this rule is that sliding skirts or other devices that by design, fabrication or as a consequence of moving, contact the track surface are prohibited and any unintended contact with the ground which either causes damage, or in the opinion of the 'dynamic event organizers' could result in damage to the track, will result in forfeit of a run or an entire dynamic event

T6.3 Wheels

T6.3.1 The wheels of the car must be 203.2 mm (8.0 inches) or more in diameter.

T6.3.2 Any wheel mounting system that uses a single retaining nut must incorporate a device to retain the nut and the wheel in the event that the nut loosens. A second nut ("jam nut") does not meet these requirements.

T6.3.3 Standard wheel lug bolts are considered engineering fasteners and any modification will be subject to extra scrutiny during technical inspection. Teams using modified lug bolts or custom designs will be required to provide proof that good engineering practices have been followed in their design.

T6.3.4 Aluminum wheel nuts may be used, but they must be hard anodized and in pristine condition.

T6.4 Tires

T6.4.1 Vehicles may have two types of tires as follows:

- Dry Tires – The tires on the vehicle when it is presented for technical inspection are defined as its "Dry Tires". The dry tires may be any size or type. They may be slicks or treaded.
- Rain Tires – Rain tires may be any size or type of treaded or grooved tire provided:
  1. The tread pattern or grooves were molded in by the tire manufacturer, or were cut by the tire manufacturer or his appointed agent. Any grooves that have been cut must have documentary proof that it was done in accordance with these rules.
  2. There is a minimum tread depth of 2.4 mms (3/32 inch).

Note: Hand cutting, grooving or modification of the tires by the teams is specifically prohibited.

T6.4.2 Within each tire set, the tire compound or size, or wheel type or size may not be changed after static judging has begun. Tire warmers are not allowed. No traction enhancers may be applied to the tires after the static judging has begun.

T6.5 Steering

T6.5.1 The steering wheel must be mechanically connected to the wheels, i.e. "steer-by-wire" is prohibited *or electrically actuated steering, is prohibited.*

T6.5.2 The steering system must have positive steering stops that prevent the steering linkages from locking up (the inversion of a four-bar linkage at one of the pivots). The stops may be placed on the uprights or on the rack and must prevent the tires from contacting suspension, body, or frame members during the track events.

T6.5.3 Allowable steering system free play is limited to seven degrees (7°) total measured at the steering wheel.

T6.5.4 The steering wheel must be attached to the column with a quick disconnect. The driver must be able to operate the quick disconnect while in the normal driving position with gloves on.

T6.5.5 The steering wheel must have a continuous perimeter that is near circular or near oval, i.e. the outer perimeter profile can have some straight sections, but no concave sections. "H", "Figure 8", or cutout wheels are not allowed.

T6.5.6 In any angular position, the top of the steering wheel must be no higher than the top-most surface of the Front Hoop. See Figure 3.

T6.5.7 Steering systems using cables for actuation are not prohibited by T6.5.1 but additional documentation must be submitted. The team must submit a failure modes and effects analysis report with design details of the proposed system as part of the structural equivalency spreadsheet (SES) or structural requirements certification form (SRCF). The report must outline the analysis that was done to show the steering system will function properly, potential failure modes and the effects of each failure mode and finally failure mitigation strategies used by the team. The organizing committee will review the submission and advise the team if the design is approved. If not approved, a non-cable based steering system must be used instead.

T6.6 Jacking Point

2013 Formula Student Rules

FORMULA STUDENT

FORMULA STUDENT

2013 Formula Student Rules
INTRODUCTION

This introduction highlights some areas of the 2013 Formula SAE rules which are used by the Formula Student Competition that teams should understand and consider. This introduction only summarises parts of the rules with revised text and does not change or replace the associated rules.

Caution – Neither this introduction, nor any other summary, is a substitute for reading and understanding the Rules. The Rules are both a controlling and a reference document and should be used for those purposes. Do not attempt to design your car based on the parts of the Rules you happen to remember from the last time you read them. We cannot stress it too strongly – Read the Rules thoroughly and repeatedly.

Revised Part Designations - The designations of some of the Parts of the FSAE Rules have been revised to better indicate their contents. The new designations are:

Part A – Administrative Regulations
Part T – General Technical Requirements
Part AF – Alternate Frame Rules
Part IC – Internal Combustion Engine Vehicles
Part EV – Technical Regulations - Electric Vehicles
Part S – Static Event Regulations
Part D – Dynamic Event Regulations

Part EV - Electric Vehicles - The rules for Electric Vehicles are now common for all international competitions. Section EV is largely based on the rules for the electric classes at Formula Student (UK) and Formula Student Germany with modifications implemented following a review by an international group of electric engineering experts. Many of the EV requirements will be familiar to teams that have participated in electric competitions.

Part IC - Internal Combustion Vehicles – To simplify the rules we have separated the rules governing internal combustion vehicles from the general technical requirements.

T1.2 Steering – The steering regulations have been modified to clarify that the use of cable steering is permitted.

T3.10.4 on the location of the 95th percentile template - The location of the template in relation to the face of the pedals has been specified.

T3.31.3 SES Test Requirements – Have been updated.

T5.6 Head Restraint – The head restraint regulations have been revised and clarified.

EV1.1.2 – Maximum Voltage – During the 2013 and 2014 Formula SAE competition years the maximum permitted nominal operational voltage is designated per competition.

EV9.1 - Electrical System Form (ESF) and EV9.2 - Failure Modes and Effects Analysis (FMEA) - Teams entering an electric vehicle are required to submit a detailed ESF and an FMEA of the tractive system. Templates for these documents will be available online and must be followed.

S3.1 Business Logic Case (BLC) – Each team is required to submit a brief "business logic case" which states the primary considerations and goals that influenced their design and fabrication choices. This submission replaces the Student Activity Disclosure Form.

C5.7 - Student Activity Disclosure Form" and all associated cross references including those in A8.1 "Required Documents and Required Forms" and A8.4 "Late Submission Penalties" – The requirement to submit the "Student Activity Disclosure Form" is eliminated.

D8.20 Efficiency – As listed in the 2012 "Notice of Possible Rule Changes" the Committee has voted to replace the Fuel Economy Event with an Efficiency Event. We suggest you thoroughly study the revised rules for this event.

2013 FORMULA SAE RULES
PART T - GENERAL TECHNICAL REQUIREMENTS

ARTICLE 1: VEHICLE REQUIREMENTS & RESTRICTIONS – AS PER 2013 FSAE RULES

ARTICLE 2: GENERAL DESIGN REQUIREMENTS – AS PER 2013 FSAE RULES

ARTICLE 3: DRIVER'S CELL – AS PER 2013 FSAE RULES EXCEPT

T3.1.1 The impact attenuator will be assessed and graded as described in the Formula Student static event rules under Technical Inspection.

ARTICLE 4: COCKPIT – AS PER 2013 FSAE RULES

ARTICLE 5: DRIVERS EQUIPMENT (BELTS AND COCKPIT PADDING) – AS PER 2013 FSAE RULES

ARTICLE 6: GENERAL CHASSIS RULES – AS PER 2013 FSAE RULES EXCEPT

T6.3 Wheels

T6.3.3 Extended or composite wheel studs are prohibited

T6.4 Tyres

T6.4.3 Remoulded or re-treaded tyres are prohibited

ARTICLE 7: BRAKE SYSTEM – AS PER 2013 FSAE RULES EXCEPT

T7.10.1 All brake fluid reservoirs must be shielded from the driver with an impermeable barrier which has a thickness of at least 0.5mm

ARTICLE 8: POWERTRAIN – AS PER 2013 FSAE RULES

ARTICLE 9: AERODYNAMIC DEVICES – AS PER 2013 FSAE RULES

ARTICLE 10: COMPRESSED GAS SYSTEMS AND HIGH PRESSURE HYDRAULICS – AS PER 2013 FSAE RULES EXCEPT

T10.3 Gaseous Fuel Systems

Any gas system on the vehicle that is used as a means of propulsion or energy source (e.g. to charge a battery through a fuel cell) must comply with the following requirements:

a. Working Gas -The working gas may be flammable, but only if it is to be burned or used for the sole means of propulsion of the vehicle.

b. Cylinder Certification - The gas cylinder/tank must be of proprietary manufacture, designed and built for the pressure being used, certified by an accredited testing laboratory in the country of its origin, and labelled or stamped appropriately. The following standard for composite cylinders applies: ISO11439 for hydrogen containers or NGV1 or ECE-R110 for natural gas, methane or similar gases. In accordance to cylinder standards, cylinders found to have external defects such as abrasions or chemical corrosion must not be used.

c. Pressure Regulation- Where cylinders are interchangeable the pressure regulator must be mounted directly onto the gas cylinder/tank. If the vehicle is to be refuelled with the cylinder on-board the vehicle, the cylinder must be fitted with an internal solenoid, supplied by Dynetek or Teleflex GFI, this must be followed by an excess flow valve prior to fitting of a regulator. The inlet to

Appendix D

Friction coefficient for dry and wet road

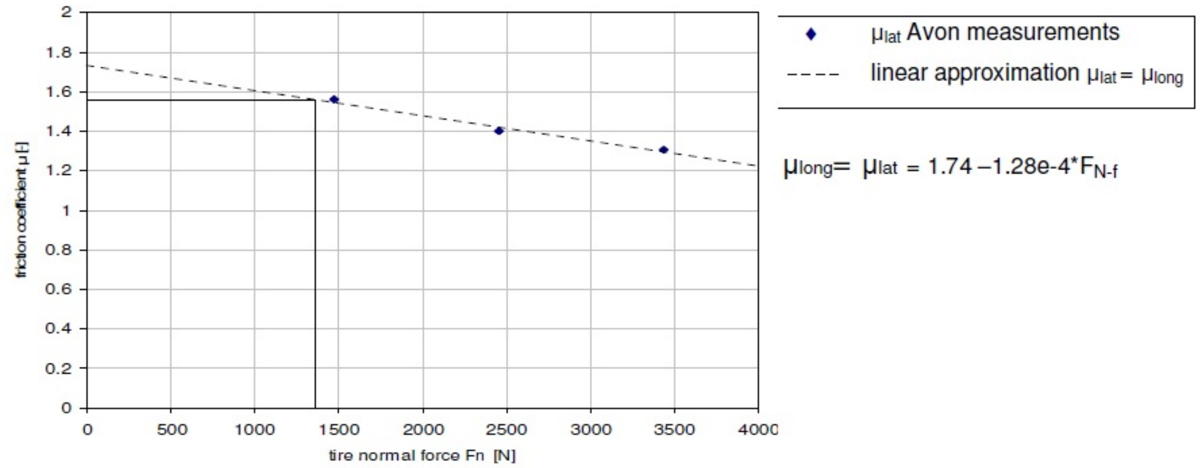

Figure D.1: dry road

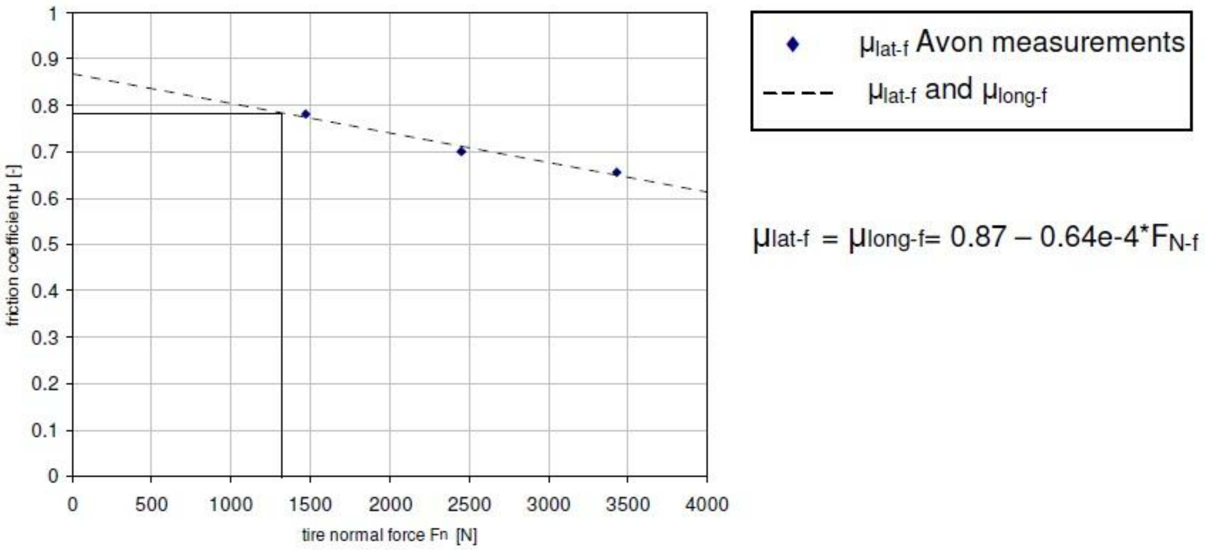

Figure D.2: wet road

Appendix E

Offset arm drawing

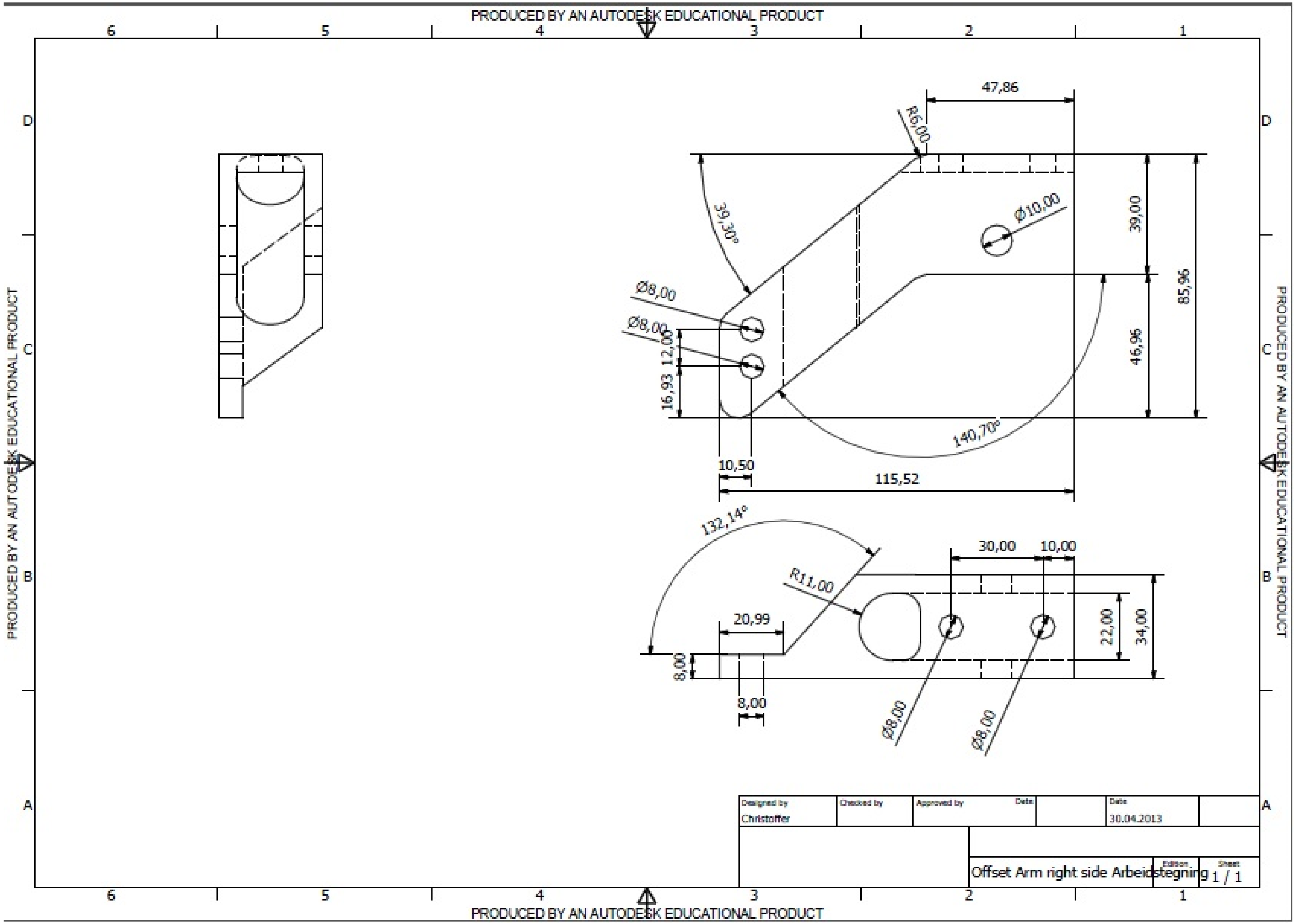

Figure E.1: Right offset arm

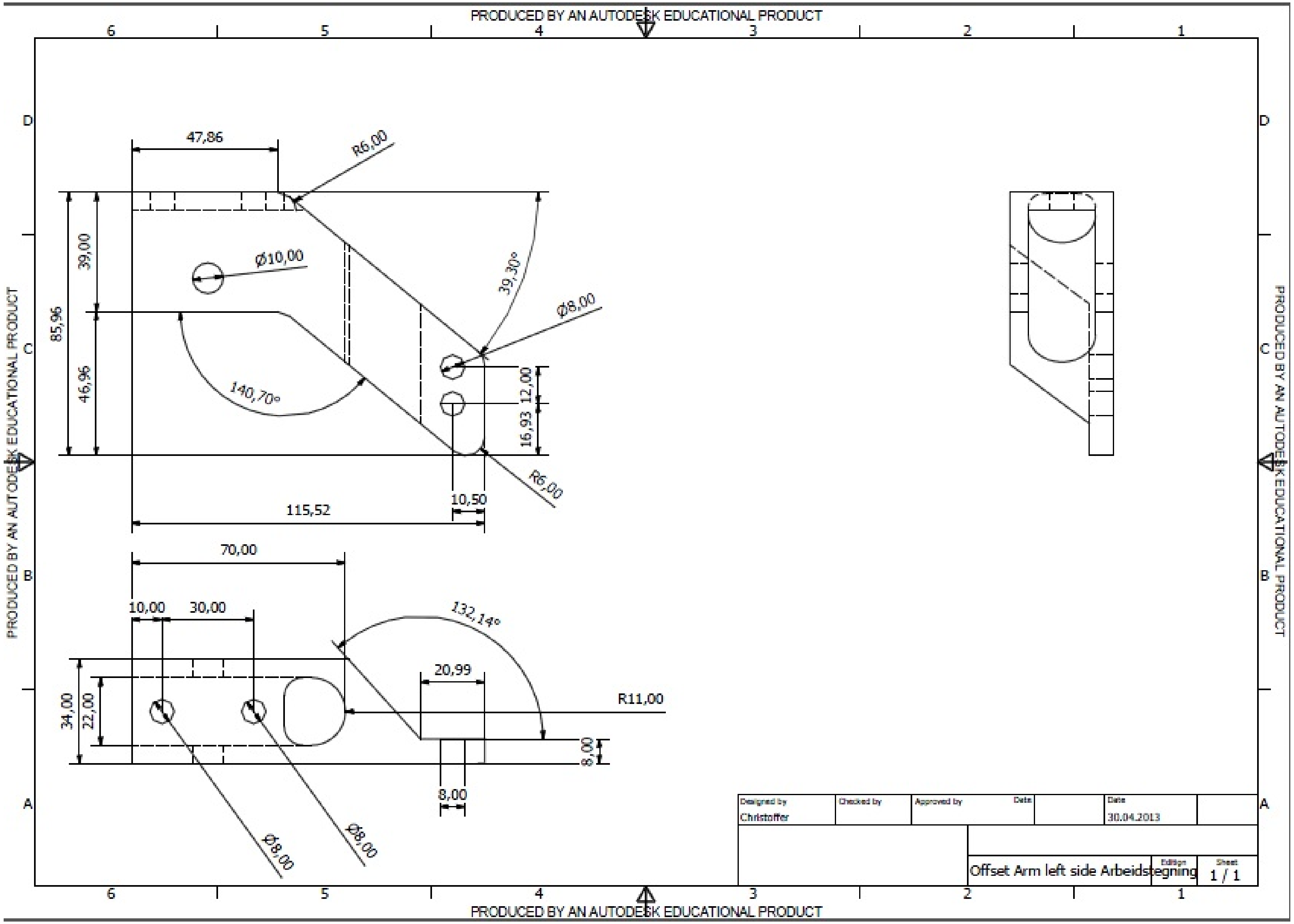

Figure E.2: Left offset arm

Appendix F

Slip angles VS cornering force and slip angle VS self-aligning torque

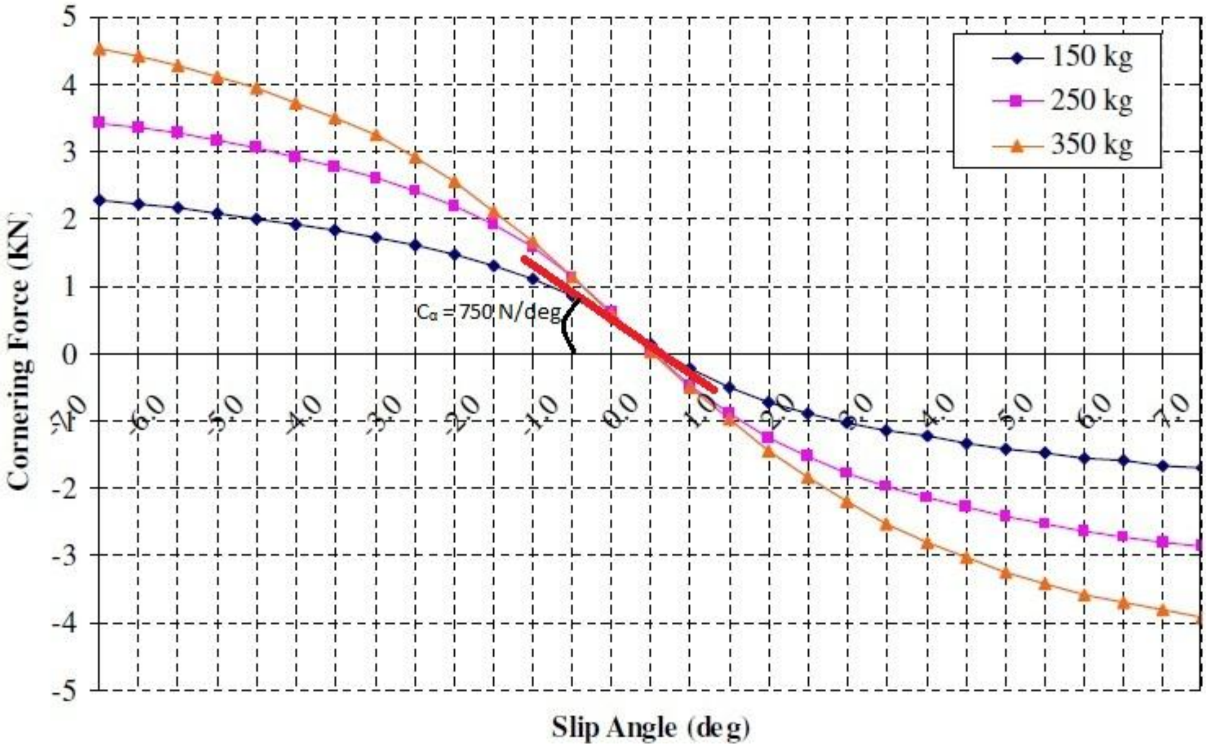

Figure F.1: Cornering stiffness C_α at a normal force of 1500 N

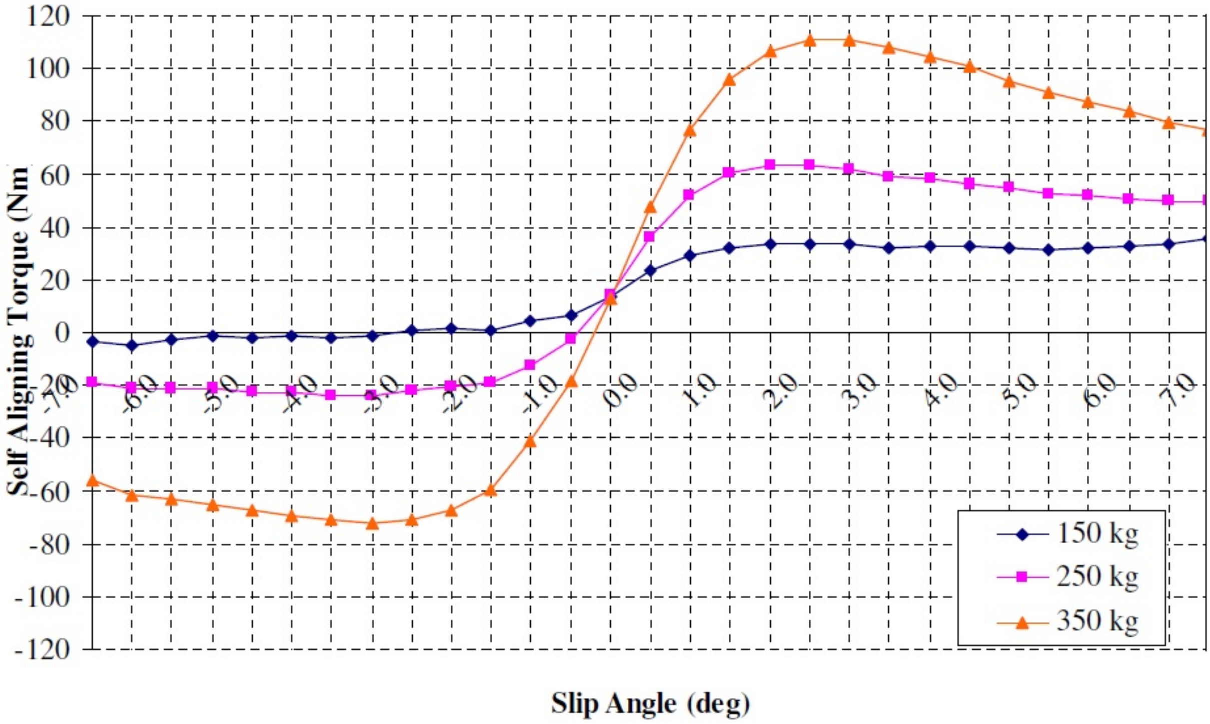

Figure F.2: Self aligning torque VS slip angle

Appendix G

Position of the steering rack

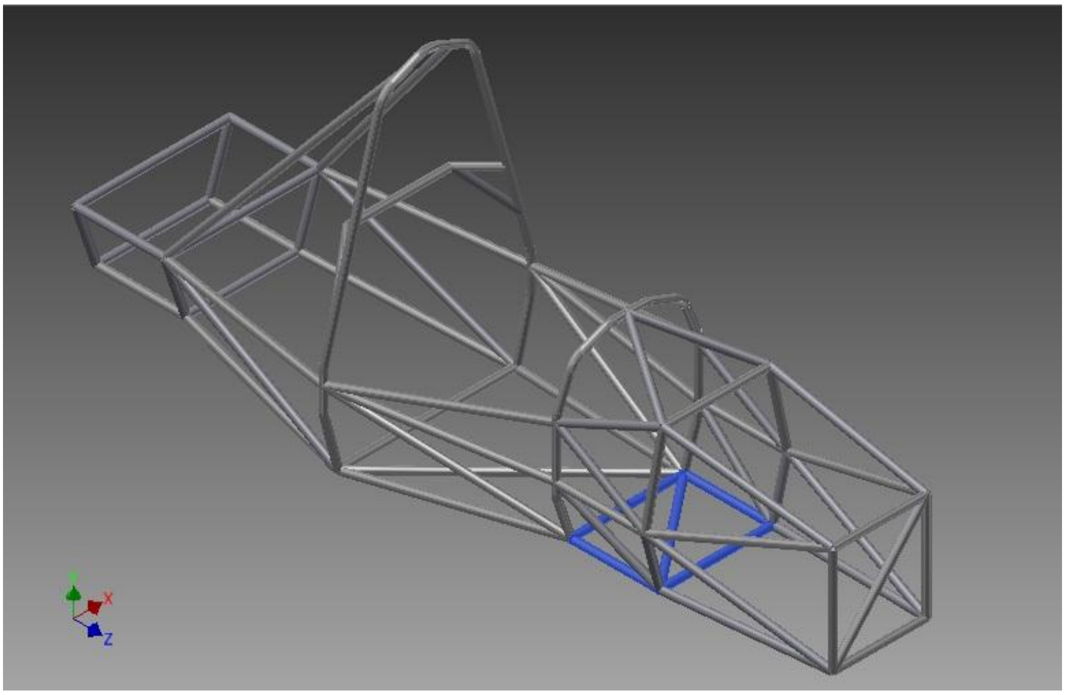

Figure G.1: The area of the frame where the steering rack may be placed

Appendix H

SKF Rod ends

Maintenance-free rod ends, male thread
Product information

Tolerances , see also text
Radial internal clearance, see also text
- Steel/sinter bronze composite
- Steel/PTFE fabric
- Steel/PTFE composite

Principal dimensions						Angle of tilt	Basic load ratings		Mass	Designation
d	d_2 max	B	G 6g	C_1 max	h	±	dynamic C	static C_0		Rod end with right or left-hand thread
mm						degrees	kN		kg	-
5	19	8	M 5	6	33	13	3,25	5,3	0,014	SAKB 5 F
5	19	8	M 5	6	33	13	3,25	5,3	0,014	SALKB 5 F
6	21	9	M 6	6,75	36	13	4,25	6,8	0,021	SAKB 6 F
6	21	9	M 6	6,75	36	13	4,25	6,8	0,021	SALKB 6 F
6	22	6	M 6	4,5	36	13	3,6	8,15	0,015	SA 6 C
6	22	6	M 6	4,5	36	13	3,6	8,15	0,015	SAL 6 C
8	25	8	M 8	6,5	42	15	5,85	12,9	0,029	SA 8 C
8	25	8	M 8	6,5	42	15	5,85	12,9	0,029	SAL 8 C
8	25	12	M 8	9	42	14	7,1	10	0,035	SAKB 8 F
8	25	12	M 8	9	42	14	7,1	10	0,035	SALKB 8 F
10	29	14	M 10	10,5	48	13	9,8	12,5	0,059	SAKB 10 F
10	29	14	M 10	10,5	48	13	9,8	12,5	0,059	SALKB 10 F
10	30	9	M 10	7,5	48	12	8,65	18,3	0,049	SA 10 C
10	30	9	M 10	7,5	48	12	8,65	18,3	0,049	SAL 10 C
12	33	16	M 12	12	54	13	13,2	15	0,093	SAKB 12 F
12	33	16	M 12	12	54	13	13,2	15	0,093	SALKB 12 F
12	35	10	M 12	8,5	54	10	11,4	24,5	0,071	SA 12 C
12	35	10	M 12	8,5	54	10	11,4	24,5	0,071	SAL 12 C
14	37	19	M 14	13,5	60	16	17	25,5	0,14	SAKB 14 F
14	37	19	M 14	13,5	60	16	17	25,5	0,14	SALKB 14 F
15	41	12	M 14	10,5	63	8	18	34,5	0,13	SA 15 C
15	41	12	M 14	10,5	63	8	18	34,5	0,13	SAL 15 C
16	43	21	M 16	15	66	15	21,4	34,5	0,21	SAKB 16 F
16	43	21	M 16	15	66	15	21,4	34,5	0,21	SALKB 16 F
17	47	14	M 16	11,5	69	10	22,4	42,5	0,19	SA 17 C

Figure H.1: Different rod ends dimensions from SKF

Maintenance-free rod ends, male thread, steel/sinter bronze composite
Product information

Tolerances , see also text
Radial internal clearance, see also text
- Steel/sinter bronze composite
- Steel/PTFE fabric
- Steel/PTFE composite

Principal dimensions						Angle of tilt	Basic load ratings		Mass	Designation
d	d_2 max	B	G 6g	C_1 max	h	±	dynamic C	static C_0		Rod end with right or left-hand thread
mm						degrees	kN		kg	-
8	25	8	M 8	6,5	42	15	5,85	12,9	0,029	SA 8 C

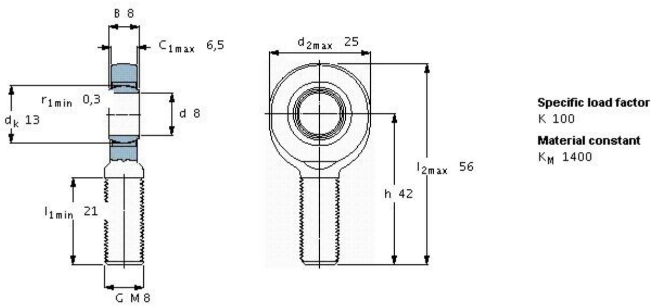

Figure H.2: 8 mm Rod end used in the steering system

Appendix I

Steel products from Aerocom with test report

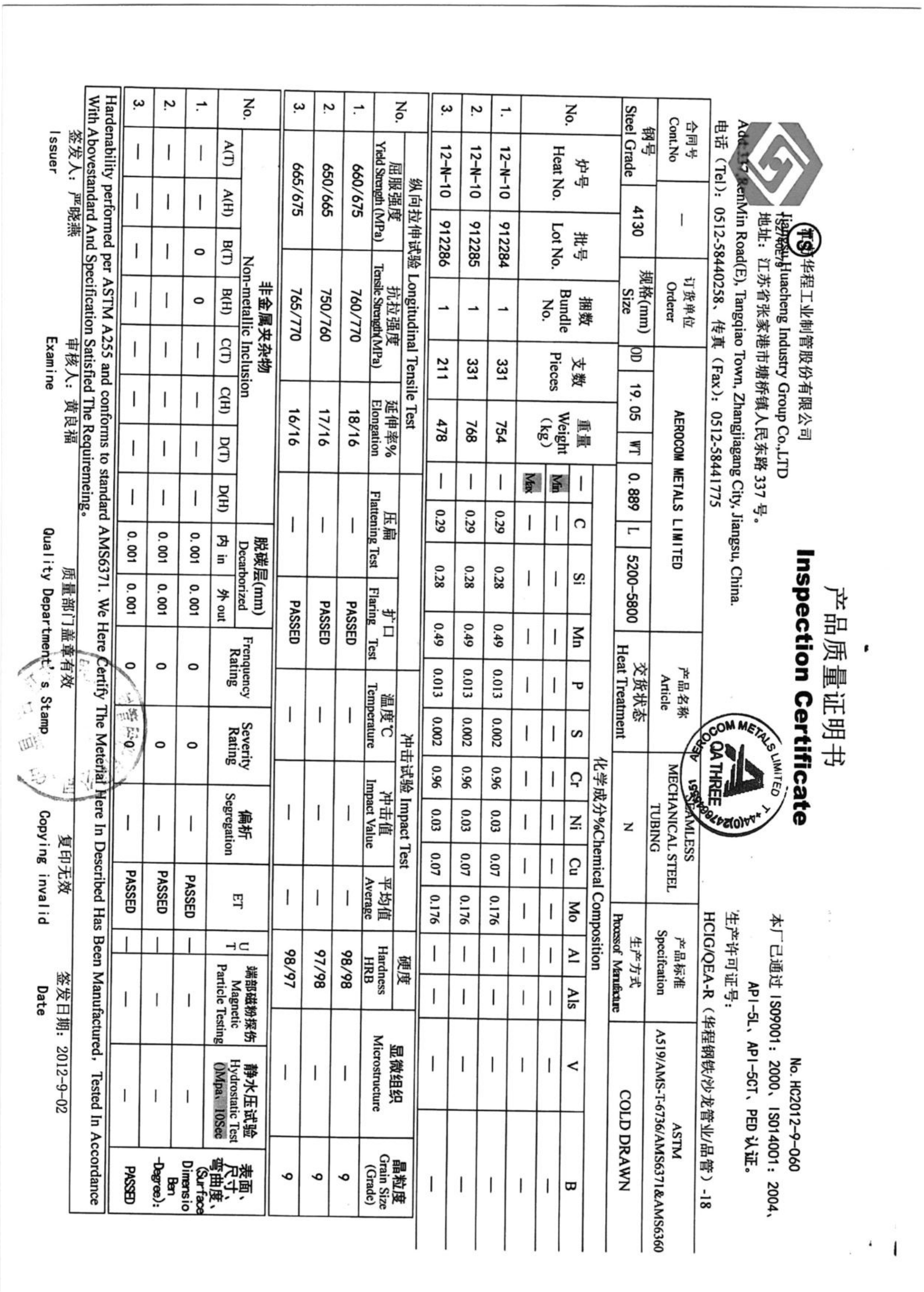

产品质量证明书

Inspection Certificate

华程工业制管股份有限公司
Jiangsu Huacheng Industry Group Co.,LTD
TS2740279
地址：江苏省张家港市塘桥镇人民东路 337 号。
Add: 337 RenMin Road(E), Tangqiao Town, Zhangjiagang City, Jiangsu, China.
电话（Tel）：0512-58440258、传真（Fax）：0512-58441775

AEROCOM METALS LIMITED QA THREE

No. HC2012-9-060
本厂已通过 ISO9001：2000、ISO14001：2004、API-5L、API-5CT、PED 认证。
生产许可证号：
HCIG/QEA-R（华程钢铁/沙龙管业/品管）-18

合同号 Cont.No	—	订货单位 Orderer	AEROCOM METALS LIMITED					产品名称 Article	SEAMLESS MECHANICAL STEEL TUBING	产品标准 Specifcation	ASTM A519/AMS-T-6736/AMS6371&AMS6360
钢号 Steel Grade	4130	规格(mm) Size	OD	19.05	WT	0.889	L 5200-5800	交货状态 Heat Treatment	N	生产方式 Processof Manufacture	COLD DRAWN

No.	炉号 Heat No.	批号 Lot No.	捆数 Bundle No.	支数 Pieces	重量 Weight (kg)	—	C	Si	Mn	P	S	Cr	Ni	Cu	Mo	Al	Als	V	B
						Min	—	—	—	—	—	—	—	—	—	—	—	—	—
						Max	—	—	—	—	—	—	—	—	—	—	—	—	—
1.	12-N-10	912284	1	331	754	—	0.29	0.28	0.49	0.013	0.002	0.96	0.03	0.07	0.176	—	—	—	—
2.	12-N-10	912285	1	331	768	—	0.29	0.28	0.49	0.013	0.002	0.96	0.03	0.07	0.176	—	—	—	—
3.	12-N-10	912286	1	211	478	—	0.29	0.28	0.49	0.013	0.002	0.96	0.03	0.07	0.176	—	—	—	—

化学成分%Chemical Composition

No.	纵向拉伸试验 Longitudinal Tensile Test					冲击试验 Impact Test			硬度	显微组织 Microstructure	晶粒度 Grain Size (Grade)
	屈服强度 Yield Strength (MPa)	抗拉强度 Tensile Strength(MPa)	延伸率% Elongation	压扁 Flattening Test	扩口 Flaring Test	温度℃ Temperature	冲击值 Impact Value	平均值 Average	Hardness HRB		
1.	660/675	760/770	18/16	—	PASSED	—	—	—	98/98	—	9
2.	650/665	750/760	17/16	—	PASSED	—	—	—	97/98	—	9
3.	665/675	765/770	16/16	—	PASSED	—	—	—	98/97	—	9

No.	非金属夹杂物 Non-metallic Inclusion								脱碳层(mm) Decarborized		Frenquency Rating	Severity Rating	偏析 Segregation	ET	UT	端部磁粉探伤 Magnetic Particle Testing	静水压试验 Hydrostatic Test ()Mpa、10Sec	表面、尺寸、弯曲度、(Surface Dimensio Ben -Degree):
	A(T)	A(H)	B(T)	B(H)	C(T)	C(H)	D(T)	D(H)	内 in	外 out								
1.	—	—	0	0	—	—	—	—	0.001	0.001	0	0	—	PASSED	—	—	—	PASSED
2.	—	—	—	—	—	—	—	—	0.001	0.001	0	0	—	PASSED	—	—	—	
3.	—	—	—	—	—	—	—	—	0.001	0.001	0	0	—	PASSED	—	—	—	

Hardenability performed per ASTM A255 and conforms to standard AMS6371. We Here Certify The Meterial Here In Described Has Been Manufactured, Tested In Accordance With Abovestandard And Specification Satisfied The Requiremeing。

签发人：严晓燕 Issuer　审核人：黄良福 Examine　质量部门盖章有效 Quality Department's Stamp　复印无效 Copying invalid　签发日期：2012-9-02 Date

Figure I.1: Inspection certificate

..angsu Huacheng Industry Pipe Making Corporation

337 Renmin Road(E),Tangqiao Town,Zhangjiagang City,Jiangsu Province(215611),P.R. of China
Tel:(86)-512-58439008 Fax:(86)-512-58439033

Mill Test Report

HCSS10-324

To: Salem Steel North America. LLC
225 Passaic Street,
Passaic NJ 07055

P.O. NO.: H10046
Invoice No.: H10052-1/3
Date:AUGUST 10, 2010

Description of goods: SEAMLESS COLD DRAWN MECHANICAL TUBING

Specification: AMS-T-6736A,Condition N,MIL-T-6736B, Condition N, AMS-6360L,AMS-6371J,A519-03,Steel Grade 4130

Physical condition: Stress Relief Annealed, and the final annealing temperature was 1150 F.

Heat No:X10902543

Chemical analysis: %

C	Mn	Si	S	P	Cr	Mo	Ni	Cu	Al	Pb	V	Ti	Sn
0.3	0.58	0.24	0.005	0.017	0.98	0.18	0.01	0.02	--	--	--	--	--

Raw material was produced by Nanjing Steel Group-Jiangsu Huai Steel Co., Ltd, P.R.China

TagNo.10046-1-5

Mechanical Properties:

Item No.	Lot No	OD	WT	Yield	Tensile	Elong-ation	Hard-ness	Decarb.	Decarb.	Grain
		Inch	Inch	P.S.I	P.S.I	%	HRB	OD/Inch	ID/Inch	size
1	904255	0.625	0.049	95341	107224	22	99	0.001	0.001	9
				94273	106158	23	98	0.001	0.001	9

Remarks:

1. Yield is determined by using the 0.2% offset method.
2. Grain size is determined and reported by Huacheng in accordance with ASTM E112
3. The material was magnetic particle tested in accordance with AMS 2640J and/or ASTM-E-1444-01 and rated as frequency and severity rating to AMS 2301J latest revision.

Frequency Rating	Severity Rating
0	0

4. Above tubing is passed by 100% eddy current testing, and conforms to the requirements of ASTM A450.
5. The size tolerance of above tubing is measured and conforms to the specification of AMS-T-6736A,Condition N,AMS2253,AMS33529.
6. Free from mercury contamination.
7. This tubing has been produced in the P.R.China

Testing Date: AUGUST 8 2010
Signed by:
Quality manager

AEROCOM METALS LIMITED T +44(0)247 QA THREE

OCT-03-2012 10:42 AM C. T. VOGELSONG CO. 717 432 4589 P.05

Figure I.2: Test report

AEROCOM METALS LIMITED

Item Master Summary

Item ID contains t-4130, In Stock > 0.1

Category	Item ID	Item Description	Manufacturer/Model	UOM	In Stock	On Order	Committed
Tube	T-4130-0.148X0.0265	0.148"od x 0.0265"w/t	4130 N to AMS-T-6736	Feet	49.44	0.00	0.00
Tube	T-4130-0.250X0.035	0.250"od x 0.035"w/t	4130 N to AMS-T-6736 & AMS6371	Feet	38.25	0.00	0.00
Tube	T-4130-0.313X0.035	0.313"od x 0.035"w/t	4130 N to AMS-T-6736 & AMS6371	Feet	57.76	0.00	0.00
Tube	T-4130-0.313X0.049	0.313"odx0.049"w/t	4130 N to AMS T 6736 & AMS 6371	Feet	55.05	0.00	0.00
Tube	T-4130-0.375X0.035	0.375"od x 0.035"w/t	4130 N to AMS-T-6736	Feet	61.62	0.33	0.00
Tube	T-4130-0.375X0.049	0.375"od x 0.049"w/t	4130 N to AMS-T-6736	Feet	48.05	0.00	0.00
Tube	T-4130-0.375X0.083	0.375"od x 0.083"w/t	4130 N to AMS-T-6736	Feet	104.93	0.00	0.00
Tube	T-4130-0.375X0.095	0.375"od x 0.095"w/t	4130N to AMS - T - 6736 & AMS 6371	Feet	25.00	0.00	0.00
Tube	T-4130-0.438X0.035	0.4375"od x 0.035"w/t	4130N to AMS -T-6736 & AMS 6371	Feet	139.30	0.00	0.00
Tube	T-4130-0.438X0.049	0.438"od x 0.049"w/t	4130 N to AMS-T-6736	Feet	9.70	0.00	0.00
Tube	T-4130-0.438x0.095	0.4375"od x 0.095"w/t	4130N to AMS-T-6736 & AMS 6371	Feet	17.83	0.00	0.00
Tube	T-4130-0.438X0.120	0.438"od x 0.120"w/t	4130 N to AMS-T-6736	Feet	83.38	0.00	0.00
Tube	T-4130-0.500X0.028	0.500"od x 0.028"w/t	4130 N to AMS T 6736	Feet	18.97	0.00	0.00
Tube	T-4130-0.500X0.035	0.500"od x 0.035"w/t	4130 N to AMS-T-6736	Feet	1,801.61	0.00	0.00
Tube	T-4130-0.500X0.049	0.500"od x 0.049"w/t	4130 N to AMS-T-6736	Feet	1,061.92	0.50	0.00
Tube	T-4130-0.500X0.058	0.500"od x 0.058"w/t	4130 N to AMS-T-6736	Feet	1,512.30	0.00	0.00
Tube	T-4130-0.500X0.065	0.500"od x 0.065"w/t	4130 N to AMS-T-6736 & AMS6371	Feet	18.66	0.00	0.00
Tube	T-4130-0.500X0.083	0.500"od x 0.083"w/t	4130 N to AMS-T-6736 & AMS6371	Feet	48.74	0.23	0.00
Tube	T-4130-0.500X0.095	0.500"od x 0.095"w/t	4130 N to AMS-T-6736	Feet	95.00	220.00	0.00
Tube	T-4130-0.500X0.120	0.500"od x 0.120"w/t	4130 N to AMS-T-6736 & AMS6371	Feet	28.50	0.00	0.00
Tube	T-4130-0.500X0.156	0.500"od x 0.156"w/t	4130 N to AMS-T-6736 & AMS6371	Feet	221.47	0.00	0.00

16/01/13 *Aerocom Metals Limited* *1*

Category	Item ID	Item Description	Manufacturer/Model	UOM	In Stock	On Order	Committed
Tube	T-4130-0.500X0.500X0.035	0.500"sq x 0.035"w/t	4130 N to AMS-T-6736 & AMS6371	Feet	1,218.80	15,000.40	4,675.00
Tube	T-4130-0.500X0.750X0.035	0.500" x 0.750" x 0.035"w/t	4130 N to AMS-T-6736	Feet	1,127.67	0.00	0.00
Tube	T-4130-0.500X1.000X0.049	0.500" x 1.000" x 0.049"w/t	4130 N to AMS-T-6736	Feet	1,373.24	11,263.00	0.00
Tube	T-4130-0.563X0.035	0.563" od x 0.035" w/t	4130 N to AMS-T-6736 & AMS6371	Feet	26.50	0.00	0.00
Tube	T-4130-0.563X0.049	0.563"od x 0.049"w/t	4130 N to AMS-T-6736 & AMS6371	Feet	56.59	0.00	0.00
Tube	T-4130-0.563X0.065	0.563"od x 0.065"w/t	4130 N to AMS-T-6736 & AMS6371	Feet	133.20	0.00	0.00
Tube	T-4130-0.625X0.028	0.625"od x 0.028"w/t	4130 N to AMS-T-6736	Feet	893.19	0.00	0.00
Tube	T-4130-0.625X0.035	0.625"od x 0.035"w/t	4130 N to AMS-T-6736 & AMS6371	Feet	89.21	0.00	0.00
Tube	T-4130-0.625X0.049	0.625"od x 0.049"w/t	4130 N to AMS-T-6736	Feet	18.91	0.50	0.00
Tube	T-4130-0.625X0.058	0.625"od x 0.058"w/t	4130 N to AMS-T-6736 & AMS6371	Feet	9.53	0.00	0.00
Tube	T-4130-0.625X0.065	0.625"od x 0.065"w/t	4130 N to AMS-T-6736	Feet	2.64	0.00	0.00
Tube	T-4130-0.625X0.083	0.625"od x 0.083"w/t	4130 N to AMS-T-6736 & AMS6371	Feet	50.66	0.00	0.00
Tube	T-4130-0.625X0.120	0.625"od x 0.120"w/t	4130 N to AMS-T-6736	Feet	60.02	0.00	0.00
Tube	T-4130-0.625X0.625X0.035	0.625"sq x 0.035"w/t	4130 N to AMS-T-6736 & AMS6371	Feet	57.00	0.00	0.00
Tube	T-4130-0.625X0.625X0.049	0.625"sq x 0.049"w/t	4130 N to AMS-T-6736 & AMS6371	Feet	157.98	0.00	0.00
Tube	T-4130-0.750X0.028	0.750"od x 0.028"w/t	4130 N to AMS-T-6736 & AMS6371	Feet	35.50	0.00	0.00
Tube	T-4130-0.750X0.035	0.750"od x 0.035"w/t	4130 N to AMS-T-6736 & AMS6371	Feet	5,505.67	16,666.30	0.00
Tube	T-4130-0.750X0.058	0.750"od x 0.058"w/t	4130 N to AMS-T-6736 & AMS6371	Feet	347.63	2,500.00	0.00
Tube	T-4130-0.750X0.065	0.750"od x 0.065"w/t	4130 N to AMS-T-6736 & AMS6371	Feet	1,235.34	2,273.00	0.00
Tube	T-4130-0.750X0.083	0.750"od x 0.083"w/t	4130 N to AMS-T-6736	Feet	19.89	0.00	0.00
Tube	T-4130-0.750X0.095	0.750"od x 0.095"w/t	4130 N to AMS-T-6736, AMS6371 & AMS6360	Feet	3,337.09	3,333.00	0.00
Tube	T-4130-0.750X0.120	0.750"od x 0.120"w/t	4130 N to AMS-T-6736	Feet	2,043.76	2,703.43	0.00
Tube	T-4130-0.750X0.156	0.750"od x 0.156"w/t	4130 N to AMS-T-6736	Feet	9.35	0.00	0.00
Tube	T-4130-0.750X0.188	0.750"od x 0.188"w/t	4130 N to AMS-T-6736 & AMS6371	Feet	8.48	0.00	0.00
Tube	T-4130-0.750X0.750X0.035	0.750"sq x 0.035"w/t	4130 N to AMS-T-6736	Feet	2,652.71	3,510.50	87.00
Tube	T-4130-0.750X0.750X0.049	0.750"sq x 0.049"w/t	4130 N to AMS-T-6736 & AMS6371	Feet	788.63	2,540.00	345.00

16/01/13 *Aerocom Metals Limited* *2*

Figure I.3: List of products from Aerocom, and chosen dimensions of steel

Appendix J

Buckling tables

TABLE 3: BUCKLING CLASS OF CROSS SECTIONS

Cross Section	Limits	Buckling about axis	Buckling Class
Rolled I-Sections 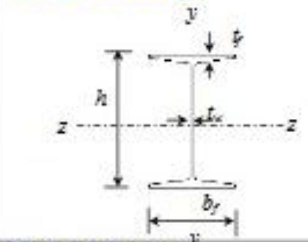	$h/b_f > 1.2$: $t_f \leq 40$ mm	z-z y-y	a b
	40 mm < $t_f \leq 100$ mm	z-z y-y	b c
	$h/b_f \leq 1.2$: $t_f \leq 100$ mm	z-z y-y	b c
	$t_f > 100$ mm	z-z y-y	d d
Welded I-Section 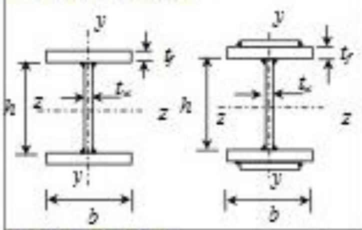	$t_f \leq 40$ mm	z-z y-y	b c
	$t_f > 40$ mm	z-z y-y	c d
Hollow Section 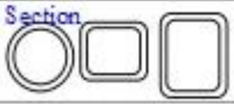	Hot rolled	Any	a
	Cold formed	Any	b
Welded Box Section 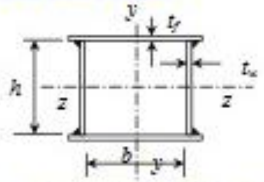	Generally (Except as below)	Any	b
	Thick welds and $b/t_f < 30$	z-z	c
	$h/t_w < 30$	y-y	c
Channel, Angle, T and Solid Sections 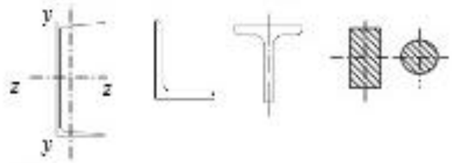		Any	c

Figure J.1: Buckling class of cross sections

TABLE 4: EFFECTIVE LENGTH OF PRISMATIC COMPRESSION MEMBERS

Boundary Conditions				Schematic representation	Effective Length
At one end		At the other end			
Translation	Rotation	Translation	Rotation		
Restrained	Restrained	Free	Free		2.0L
Free	Restrained	Restrained	Free		
Restrained	Free	Restrained	Free		1.0L
Restrained	Restrained	Free	Restrained		1.2L
Restrained	Restrained	Restrained	Free		0.8L
Restrained	Restrained	Restrained	Restrained		0.65 L

Figure J.2: Effective length of prismatic compression members

Appendix K

SKF Ball bearing specification

Principal dimensions			Basic load ratings		Speed ratings		Designation
			dynamic	static	Reference speed	Limiting speed	
d	D	B	C	C_0			* **SKF Explorer bearing**
mm			kN		r/min		-
20	42	12	9,95	5	38000	24000	**6004** *

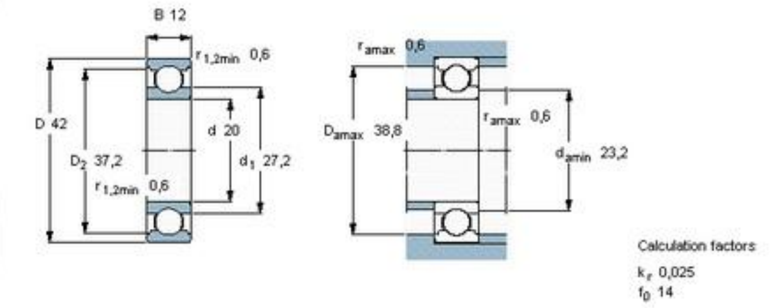

Figure K.1: Quick release axle ball bearing specifications

Appendix L

MSC Adams steering subsystem and assembly model

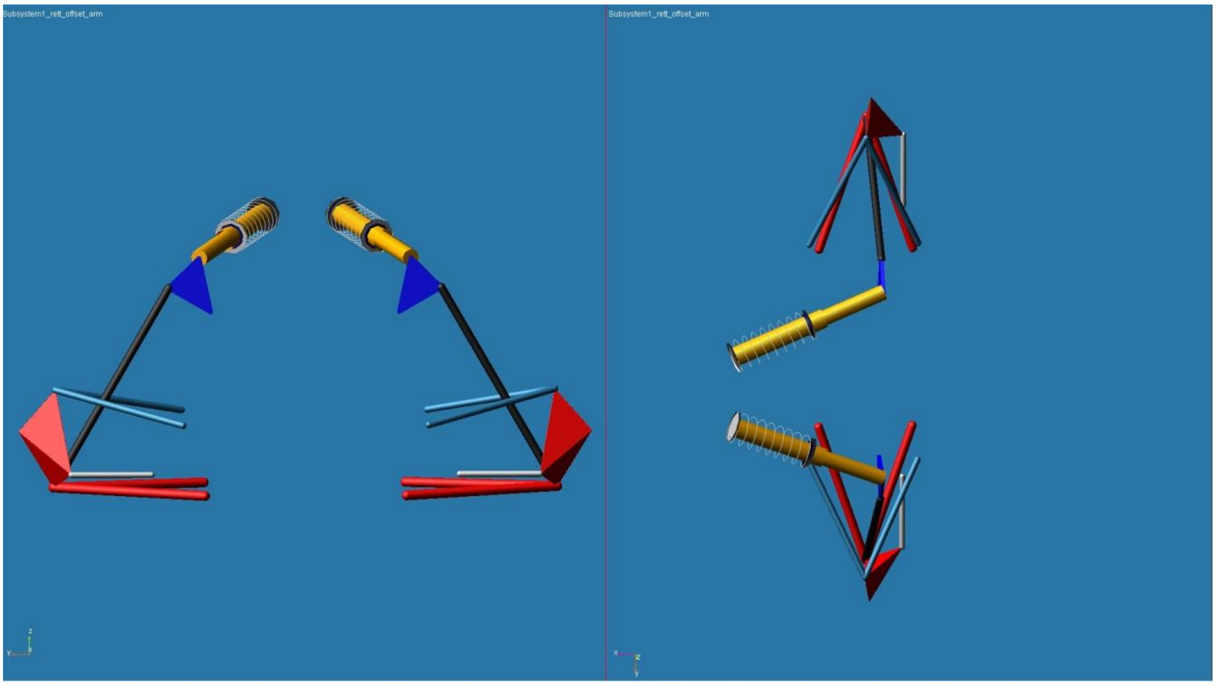

Figure L.1: Front suspension subsystem model

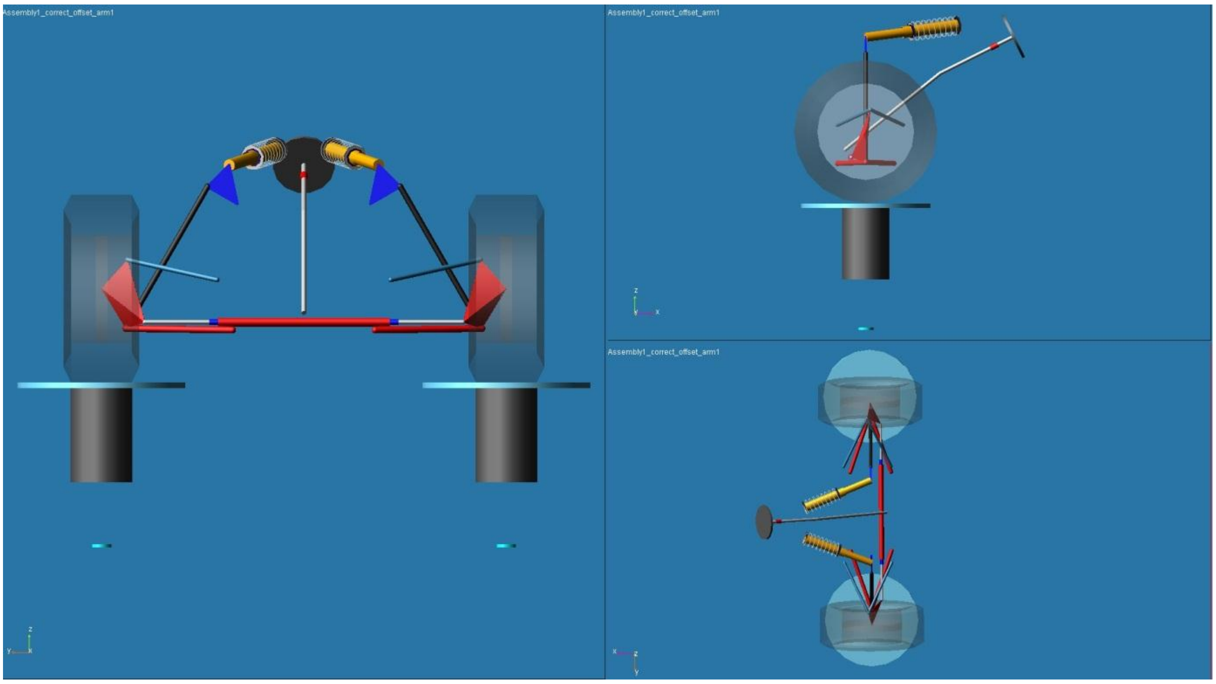

Figure L.2: Assembly with front suspension subsystem, fsae_2012 steering subsystem and test rig

Appendix M

MSC Adams analysis

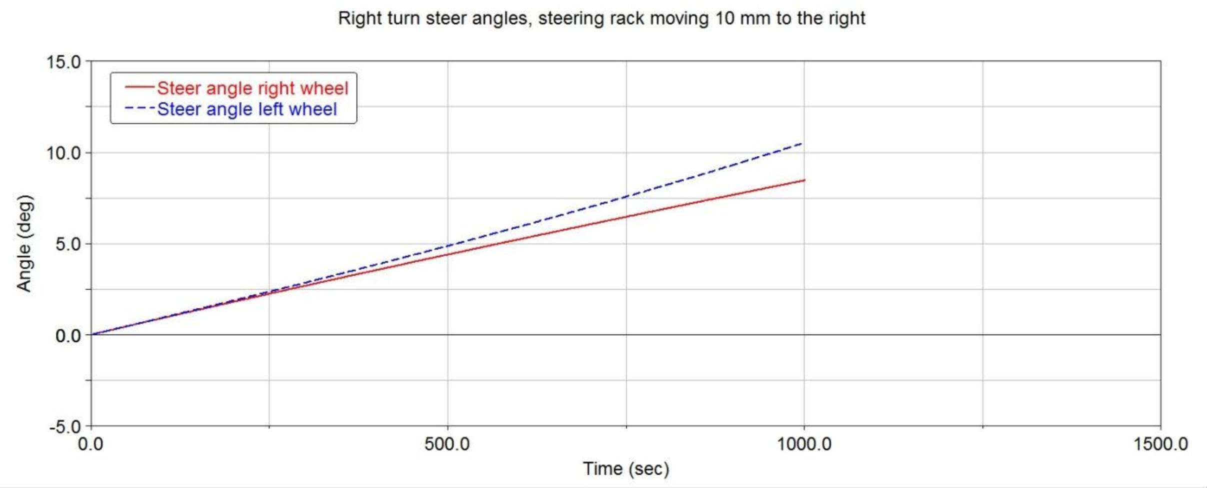

Figure M.1: Steer angles when steering rack moving 10 mm to the right

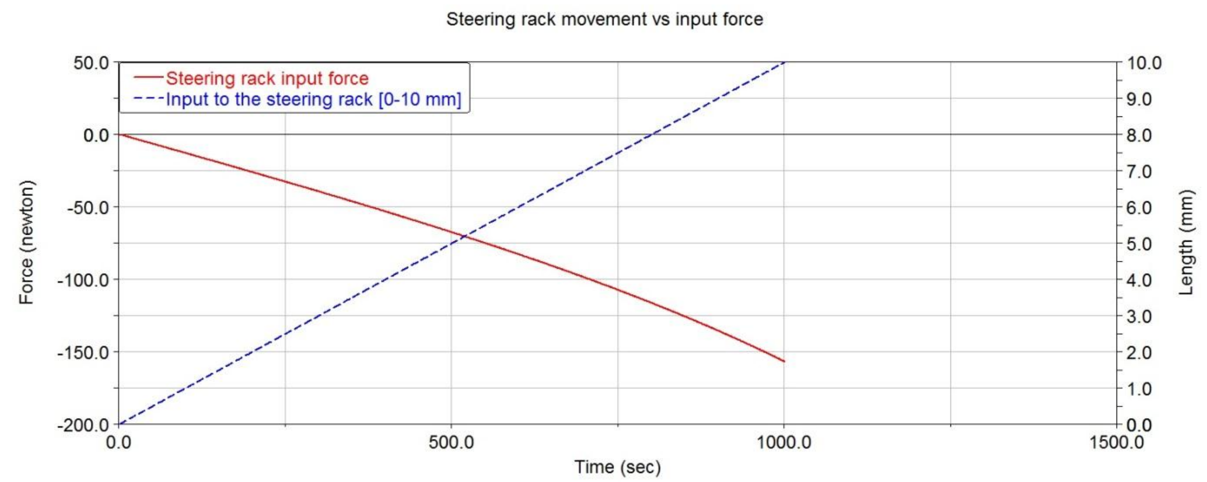

Figure M.2: Steering rack movement VS input force

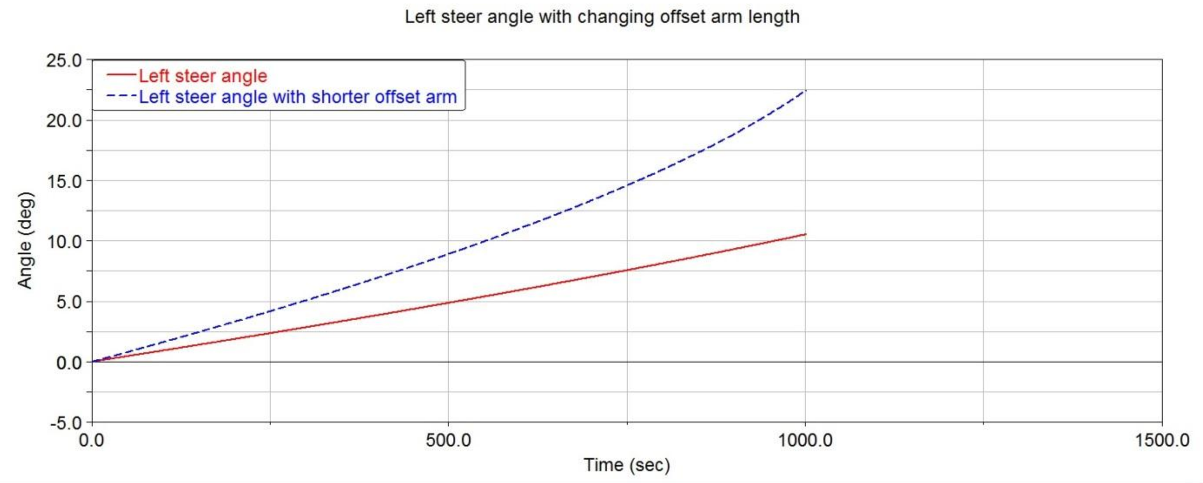

Figure M.3: Left steer angle with changing offset arm length

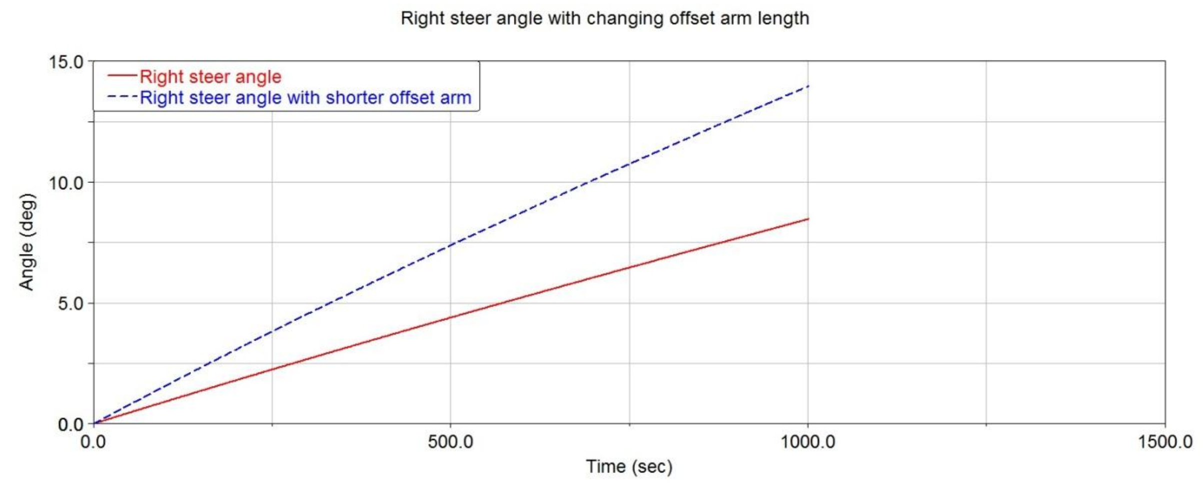

Figure M.4: Right steer angle with changing offset arm length

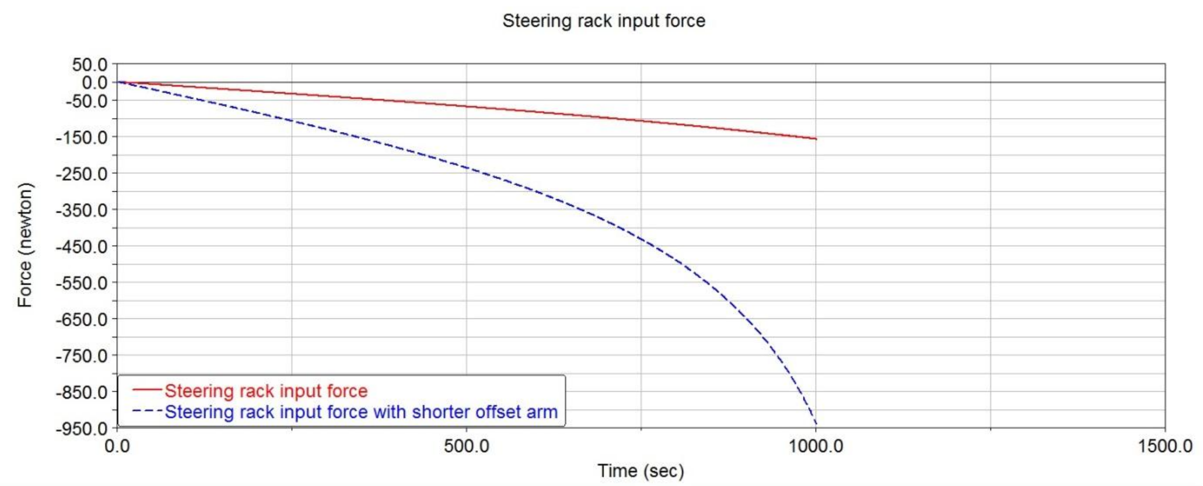

Figure M.5: Steering rack input force

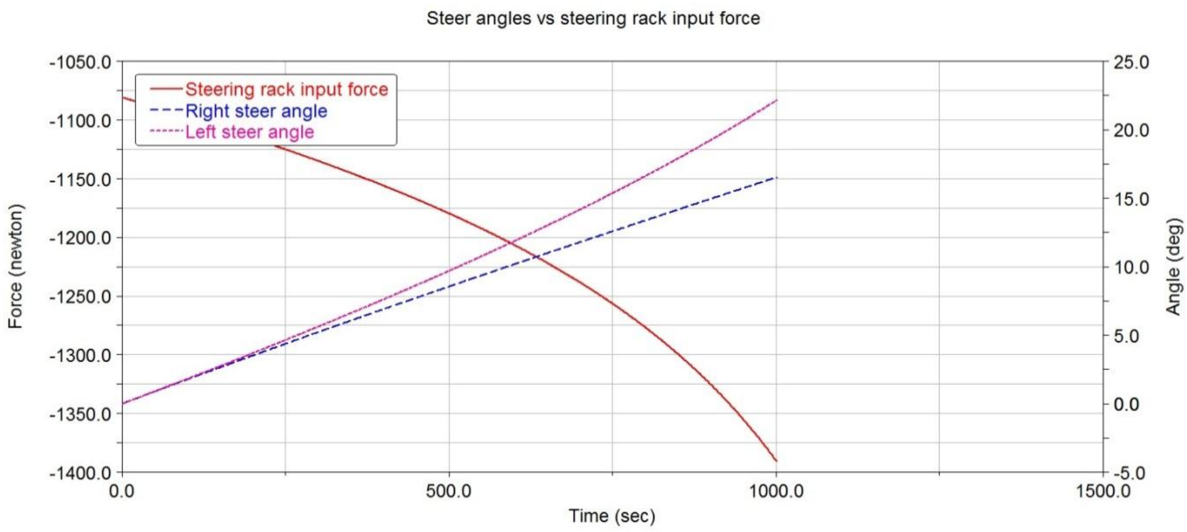

Figure M.6: Steer angles VS steering rack input force

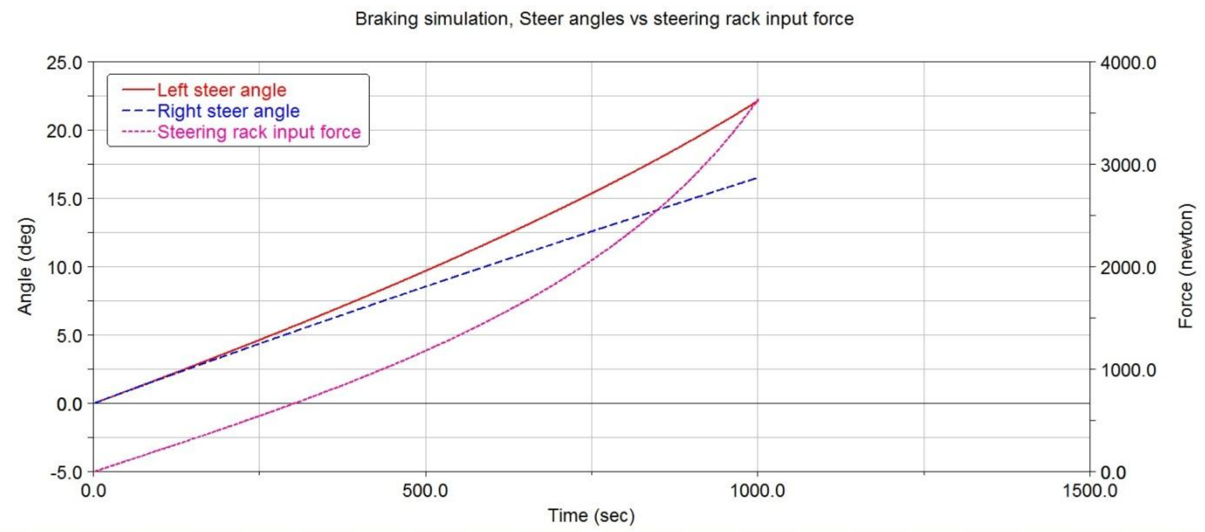

Figure M.7: Braking simulation

Appendix N

Failure Mode and Effect Analysis (FMEA)

							1/3
Failure Mode	**Failure Causes**	**Failure Effects**	**Likelihood of Occurence (1-10)**	**Likelihood of Detection (1-10)**	**Severity (1-10)**	**Risk Priority Number (RPN)**	**Actions to Reduce Occurrence of Failure**
Loose nut on bolt	Nut is not tightened securely and vibrates out of position	The system may respond slower when turning the steering wheel	*4*	*1*	*8*	*32*	Inspect and tighten the nuts after each event/test-drive
Nut fall off from bolt	Vibration when system in operation	Rod ends can disconnect from offset arm, disconnecting the wheel(s) from the system The tie rod(s) can disconnect from the system The steering wheel column can disconnect from the system Loss of control of the car Can cause serious damage and injuries if happening at high speeds and in close proximity to spectators and other drivers	*1*	*1*	*10*	*10*	Inspect and tighten the nuts after each event/test-drive Use bolts with increase length to raise the distance the nut has to travel before falling off
Failure of rod end	Failure due to wear	Increasing resistance when moving the tie rods	*2*	*3*	*4*	*24*	Inspect and clean rod ends after each event/test-drive

							2/3
Loose tie rods	Rod ends not connected properly to tie rods	Increases the amount of play on steering wheel when turning	*3*	*1*	*5*	*15*	Use lock screw to secure the right position for the rod ends
Bearing failure	Failure due to contamination	Vibrational feeling when turning the steering wheel	*2*	*3*	*4*	*24*	Keep the bearings in a protected environment If contaminated, clean the bearings Replace bearings if seal is broken
Bearing failure	Failure due to fatigue	A marked increase in vibration indicates a fatigue problem	*2*	*3*	*4*	*24*	Change the bearings after the Formula Student Season
Bearing failure	Failure due to corrosion	Failure of the bearing, increasing the resistance when turning the steering wheel	*2*	*3*	*4*	*24*	Keep the bearings in a protected environment, diverting corrosive fluids and corrosive atmosphere Inspect the seals of the bearings
Ragged motion or total failure of motion of the rack and pinion gear in steering rack	Wear on gear due to contact with contaminants or absence of lubrication	The steering rack may enter a locked position and/or not turn at all due to missing teeth on the gear, causing no turn at all. Can cause serious damage and injuries if happening at high speeds and in close proximity to spectators and other drivers	*1*	*5*	*10*	*50*	Inspect the gear after each event/test-drive Clean the gear and seal it to avoid contact with contaminations Use lubricant on the rack and pinion gear

							3/3
Quick release axle moves forward or backwards of mounted position	Set screws holding quick release mechanism in the correct position are too loose	Unable to turn the wheels as the double cross link steering wheel column will lock into position due to inadequate angles of the links Can cause serious damage and injuries if happening at high speeds and in close proximity to spectators and other drivers	*3*	*3*	*9*	*81*	Manually checking the set screws after each event/test-drive Tightening of the set screws holding the quick-release mechanism in position
Steering wheel disconnects from quick release mechanism	Steering wheel is not connected properly to quick release mechanism	Unable to turn the wheels as the steering wheel is disconnected from the system Can cause serious damage and injuries if happening at high speeds and in close proximity to spectators and other drivers	*3*	*2*	*10*	*60*	Rotate the steering wheel into locked position in quick release mechanism when connecting to the system Manually double check that the right position is maintained Use sticker to highlight the correct position when connecting
						Total RPN: ***344***	

Figure N.1: Failure mode and effect analysis

Appendix O

Cost and Weight analysis

Piece	Amount	Price/piece [NOK]	For the pieces [NOK]		Weight/piece [grams]	Weight [grams]	
Steering wheel	1	0	0		401	401	
Steering rack R4	1	1500	1500		1180	1180	
4130 Steel Hollow profile for fastening	1	0	0		76	76	
4130 Steel plate 3mm	1	0	0		197,2	197,2	
12.9 Bolts M6x70	4	9	36		16,5	66	
Nuts M6	4	1	4		2,1	8,4	
Skiver M6	4	1	4		1,1	4,4	
Steering wheel column double cross link	1	600	600		662	662	
S235 Hollow column Do=48mm, Di=42mm for quick release	1	0	0		91	91	
S235 hollow column Do=17mm, Di=13mm for quick release	1	0	0		98,4	98,4	
Quick Release	1	2211	2211		118,4	118,4	
SKF Bearing	2	106	212		67,6	135,2	
Rubber for steering rack	2	125	250		54,8	109,6	
4130 Steel for tie rods	1	263,56	263,56		117,8	235,6	
Rod end	4	217	868		30,8	123,2	
12.9 Bolts M8	4	11	44		18	72	
Nuts M8	4	1,5	6		2,2	8,8	
Skiver M8	4	1	4		1,1	4,4	
Offset Arms Aluminium	2	113	226		183,1	366,2	
Total			***6228,56***	***NOK***		***3957,8***	***grams***
Budget			***5500***	***NOK***			
Aberration			***-728,56***	***NOK***			

Figure O.1: Cost and weight analysis